

# The solar chromosphere in observations and simulations

Július Koza

Astronomical Institute  
Slovak Academy of Sciences  
Tatranská Lomnica

4<sup>th</sup> International workshop  
on small scale solar magnetic fields  
Bairisch Kölldorf, 23<sup>rd</sup> - 25<sup>th</sup> of April 2014



# The chromosphere: gateway to the corona?

The chromosphere typically requires 100 times more power than the corona.



Variable chromospheric UV influences the Earth's atmosphere.

We do not understand from first principles why the Sun is obliged to manifest spicules and fibrils.

... Or the purgatory of solar physics?

# The chromosphere in context of this workshop

Why must chromospheres exist?

“Answer”: non-radiative heating

Energy source: sub-photospheric convection, but

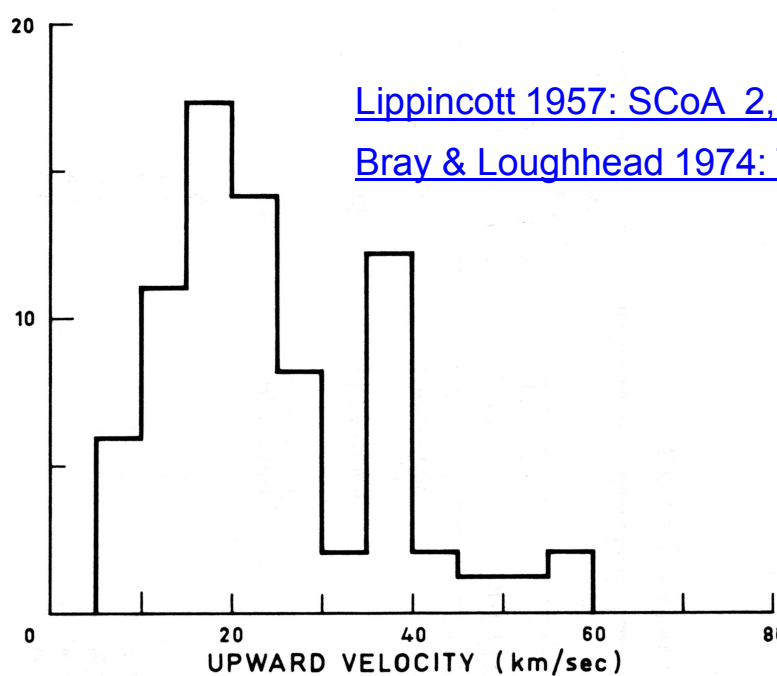
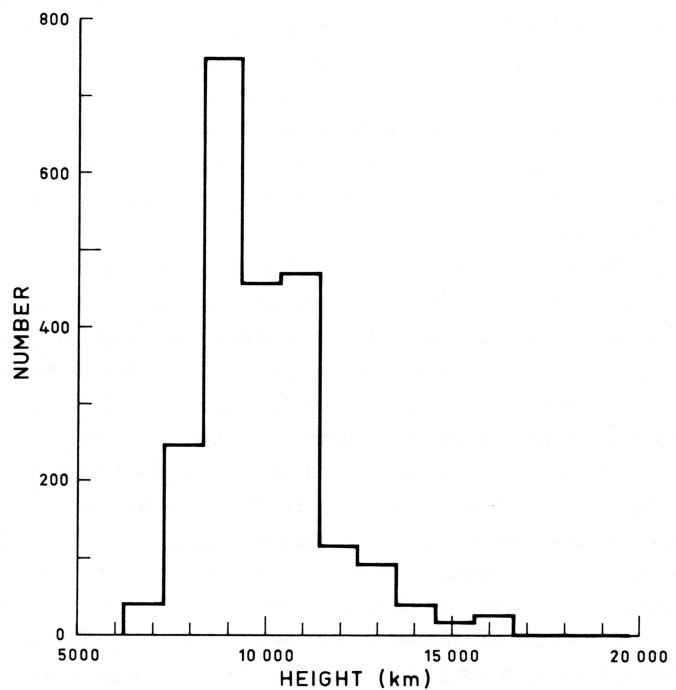
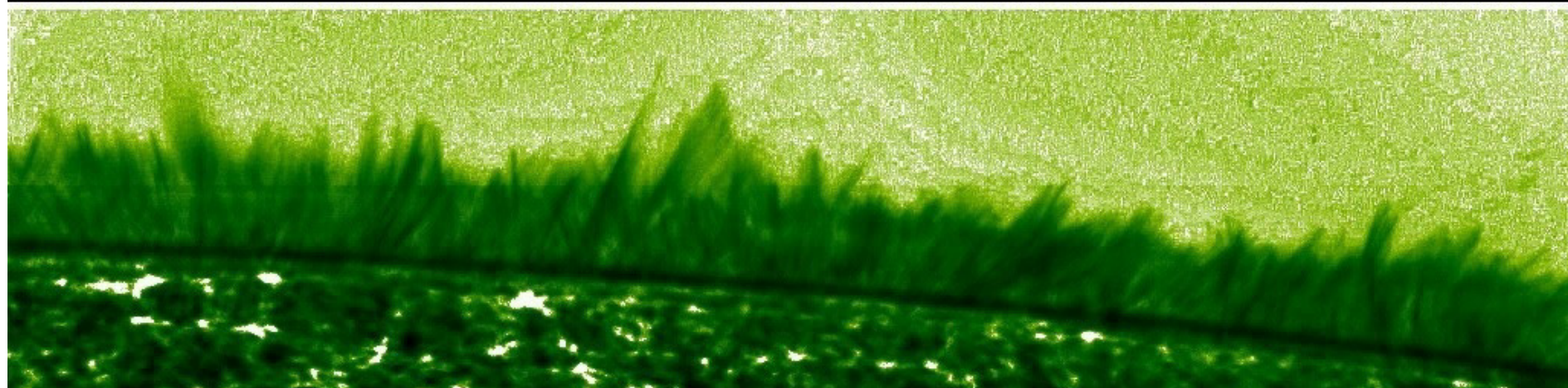
What transports energy?

What dissipates it?

We must look to magnetism for transport and dissipation of free energy. Here small-scale magnetic fields come on the stage!

# Spicules – chromospheric conundrum

2006-11-22T05:57:31.405Z

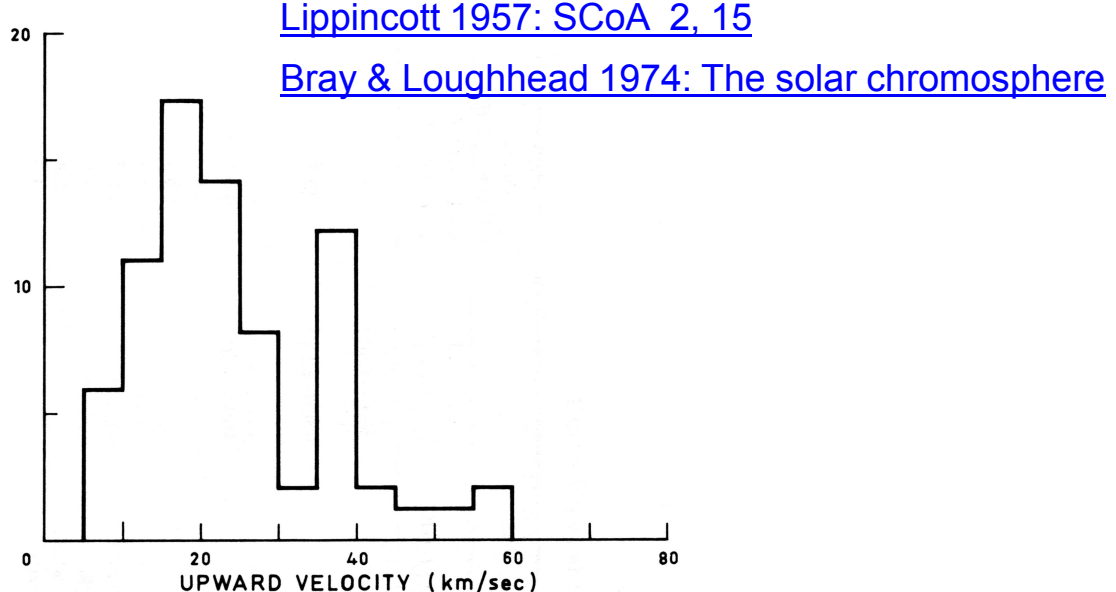
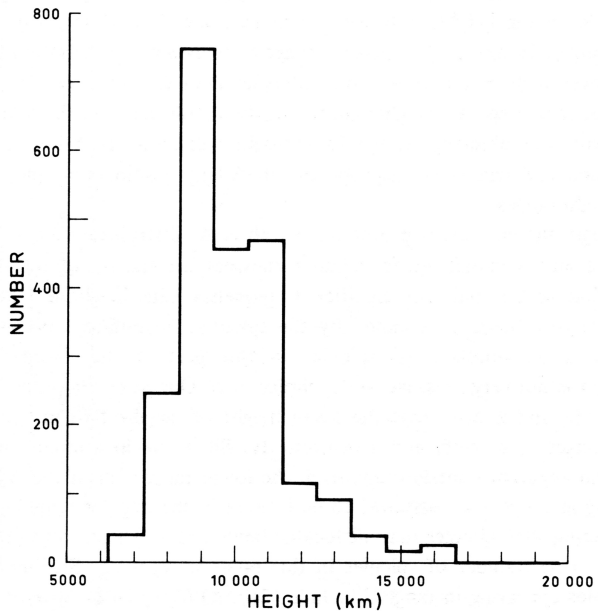


Hinode Ca II H

[Lippincott 1957: SCoA 2, 15](#)

[Bray & Loughhead 1974: The solar chromosphere](#)

# What drives spicules ?



$$\langle h_{\max} \rangle \approx 9800 \text{ km}$$

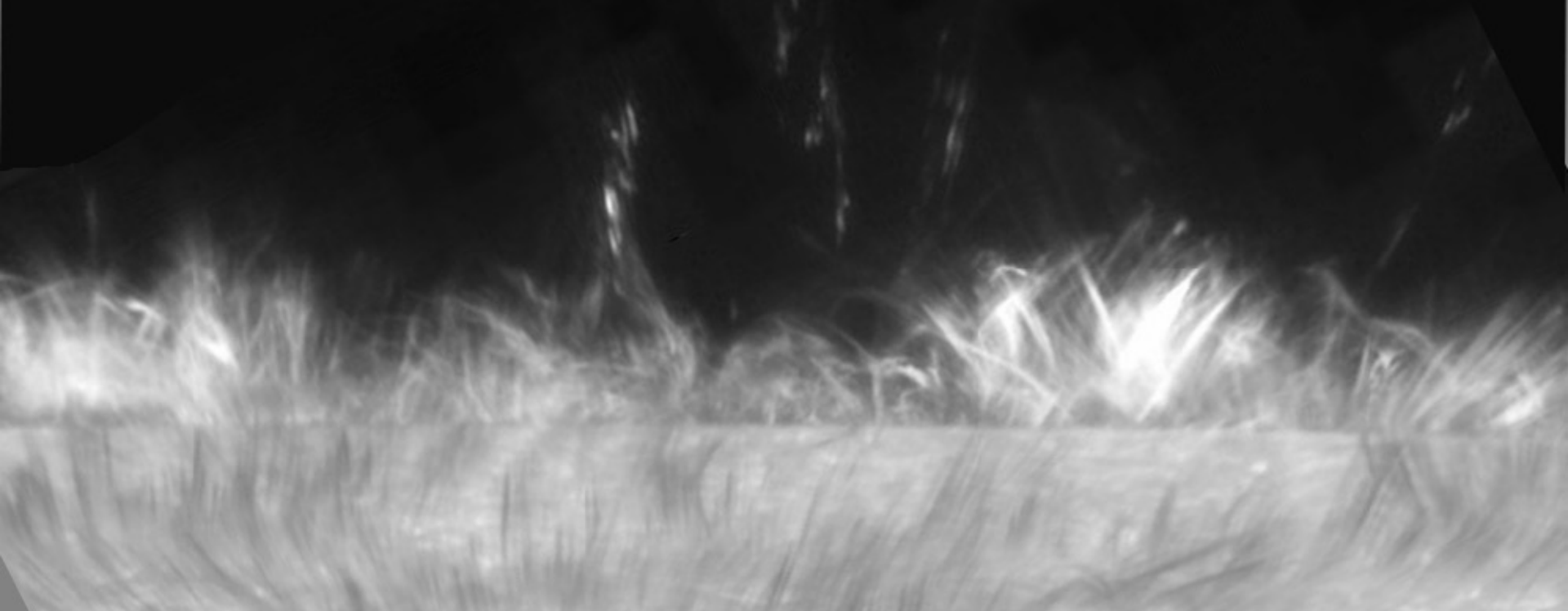
$$\langle v_{\max} \rangle \approx 24 \text{ km s}^{-1}$$

But : 
$$h_{\max} = \frac{\langle v_{\max} \rangle^2}{2g} = 1050 \text{ km}$$

$$v_{\max} = \sqrt{2g\langle h_{\max} \rangle} = 73 \text{ km s}^{-1}$$

g – solar gravity:  $274 \text{ m s}^{-2}$

Unknown driver propels spicules **much higher** than results from their **maximum velocities**, assuming an initial impulse followed by ballistic motion.



[de la Cruz Rodríguez 2010: PhD Thesis](#)

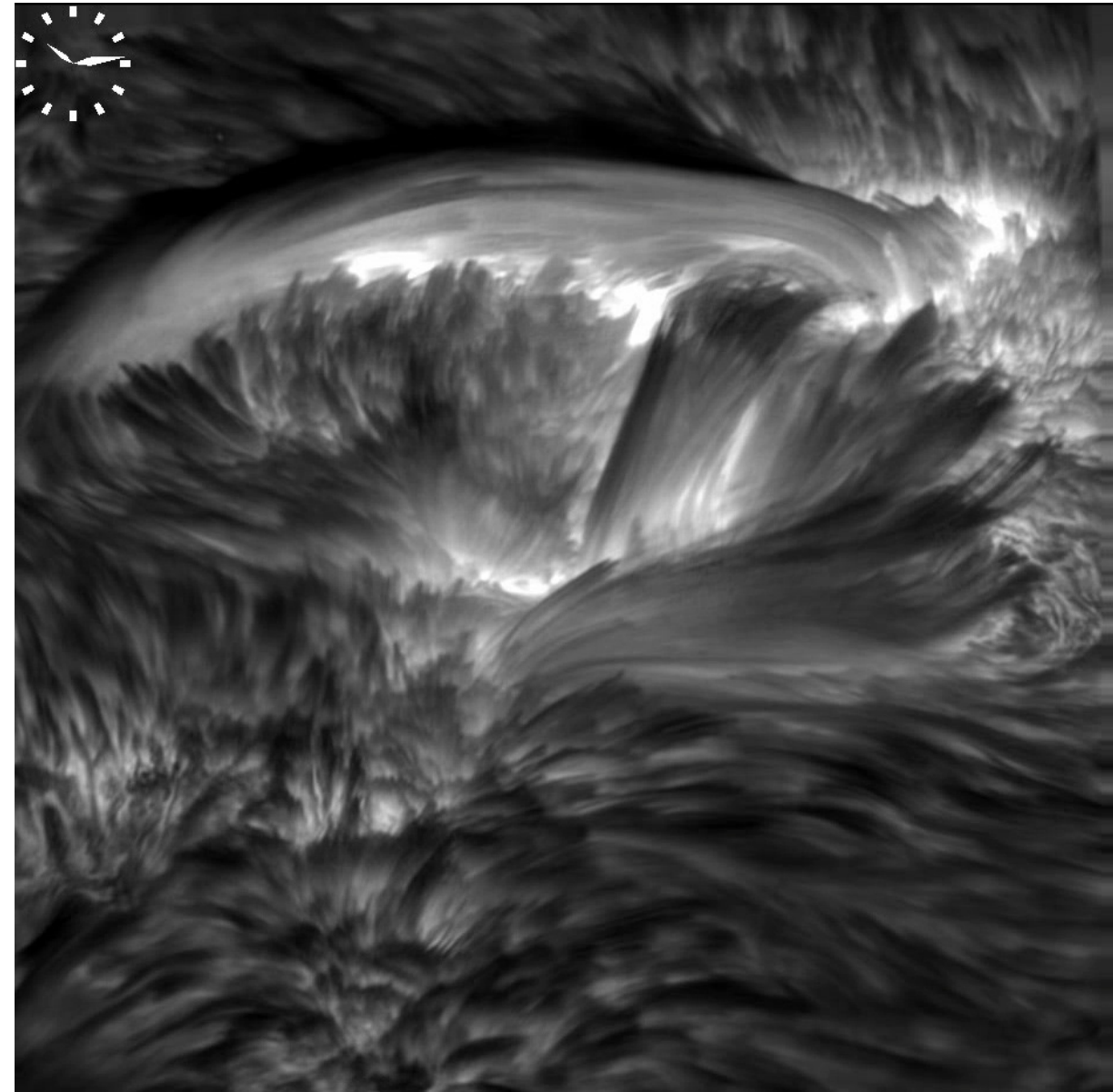
Are spicules and fibrils related to chromospheric and coronal heating?

Are they related to mass transport into corona?

Are fibrils on-disk counterparts of spicules?

What drives spicules?

# State-of-the-art imaging of the chromosphere



Swedish 1-m Solar Telescope  
+ adaptive optics  
+ MOMFBD

diagnostics: H $\alpha$  line center

date: 2005 October 4

duration: 72 min

Resolutions

temporal: 3 frames per second

spatial: ~ 70 – 100 km

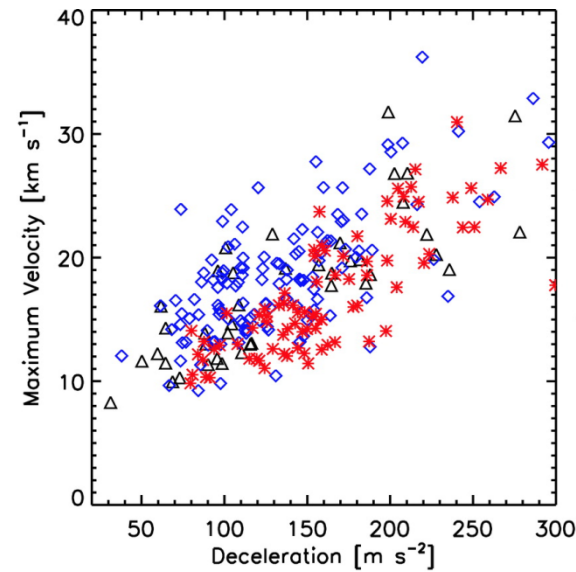
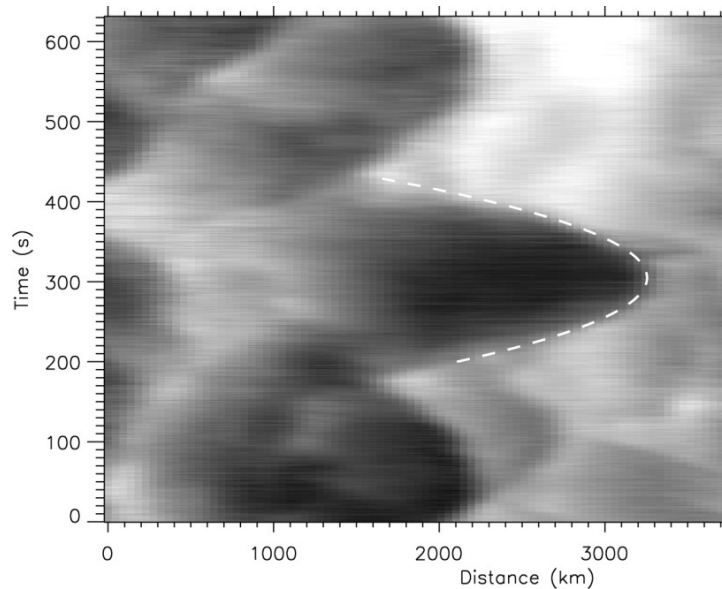
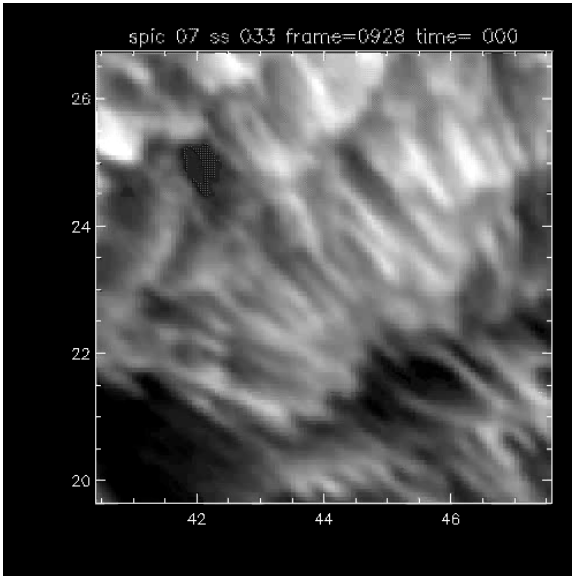
Field of view:

61 arcsec  $\times$  61 arcsec

**Main result:**

H $\alpha$  image sequence with the highest resolution ever achieved.

# Imaging of dynamic fibrils in a plage



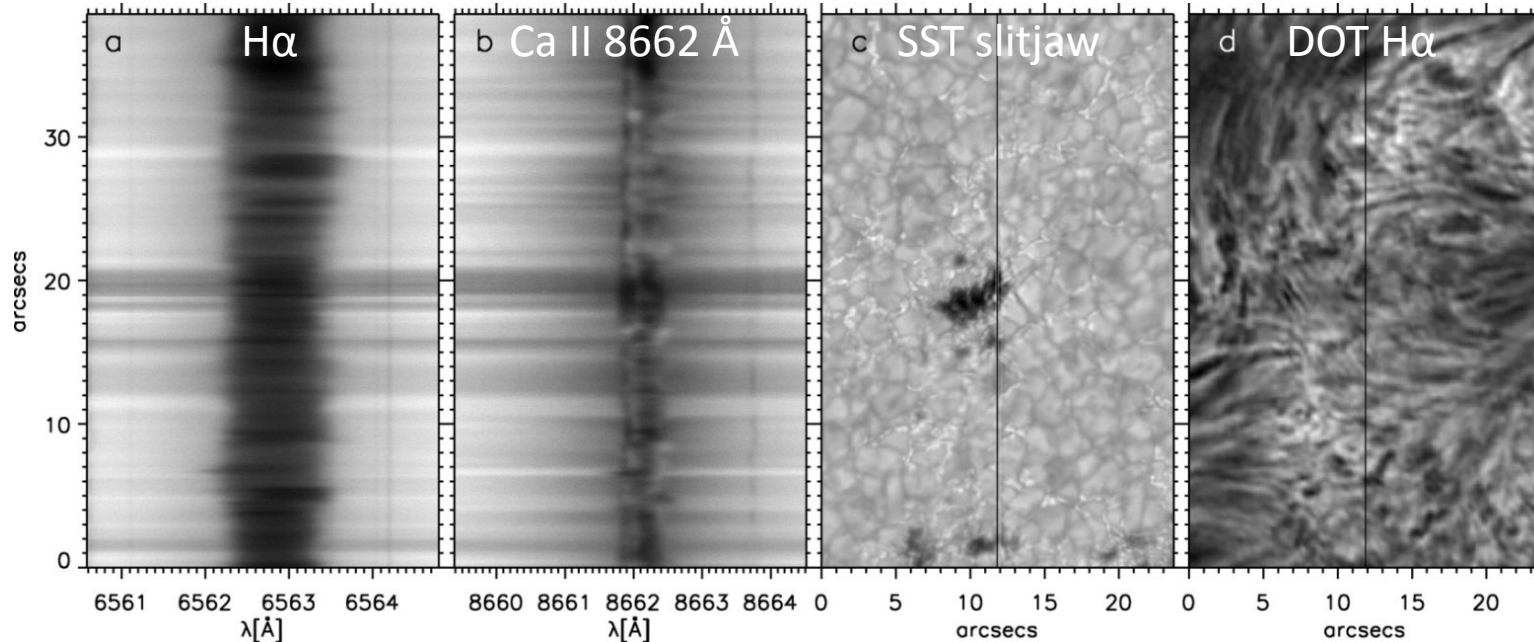
[Hansteen et al. 2006: ApJ 647, 73](#)

[De Pontieu et al. 2007: ApJ 655, 624](#)

## Main results:

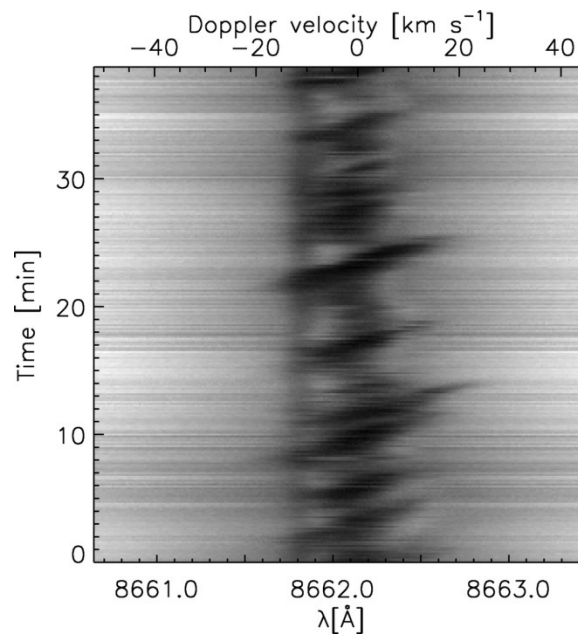
- confirmed extensions and retractions
- confirmed parabolic top trajectories
- linear relationship between maximum velocity and deceleration
- H $\alpha$  dynamic fibrils in a plage co-spatial with areas of increased power of 5-min oscillations
- field-aligned magnetoacoustic shock excitation

# Spectroscopy of dynamic fibrils



Velocity-time plot  
for Ca II 8662 Å .

Dynamic fibrils  
seen as diagonal  
dark components  
across the  
spectral line.



SST + TRIPPEL spectrograph + AO +  
DOT imaging

date: 4 May 2006

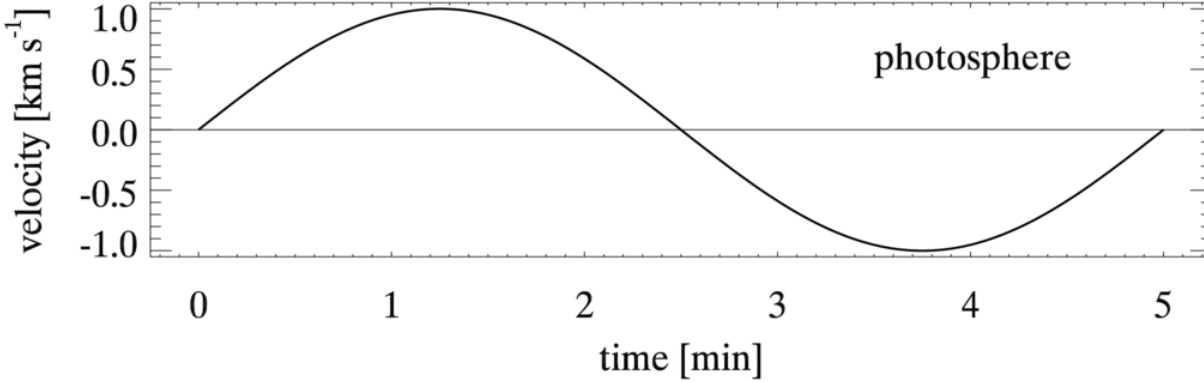
duration: 40 min

cadence: 0.5 s

## Main result:

Extensions and retractions of dynamic  
fibrils are actual mass motions.

# N-shaped magnetoacoustic shocks



acoustic cutoff period

$$P_{\text{ac}} = \frac{4\pi}{g \cos \theta} \sqrt{\frac{RT}{\gamma \mu}}$$

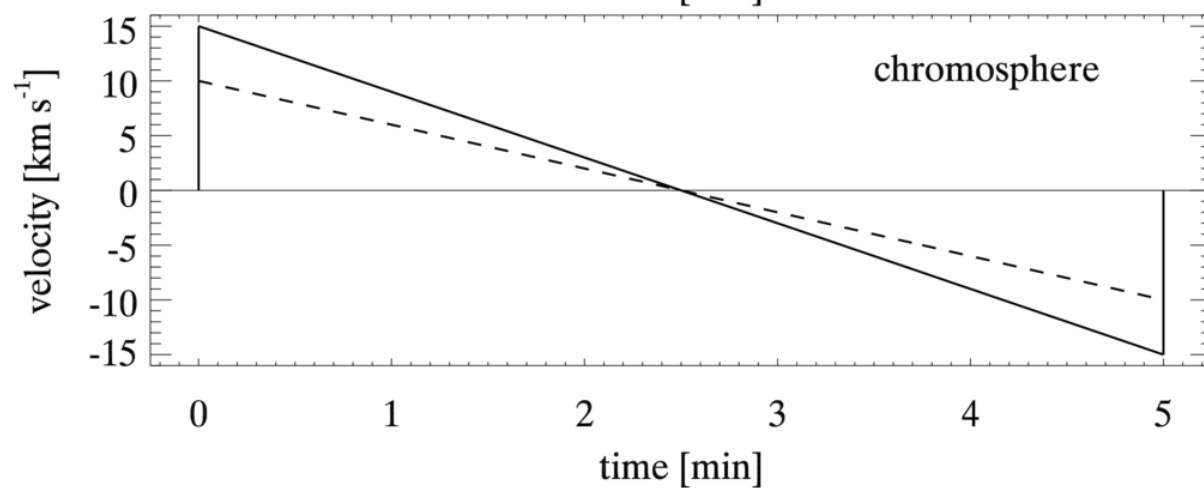
$$E_{\text{kin}} = \frac{1}{2} \rho v^2 = \text{const.}$$

from shock discontinuity to parabola

$$v = v_{\text{max}} - at$$

$$y = y_0 + v_{\text{max}}t - \frac{a}{2}t^2$$

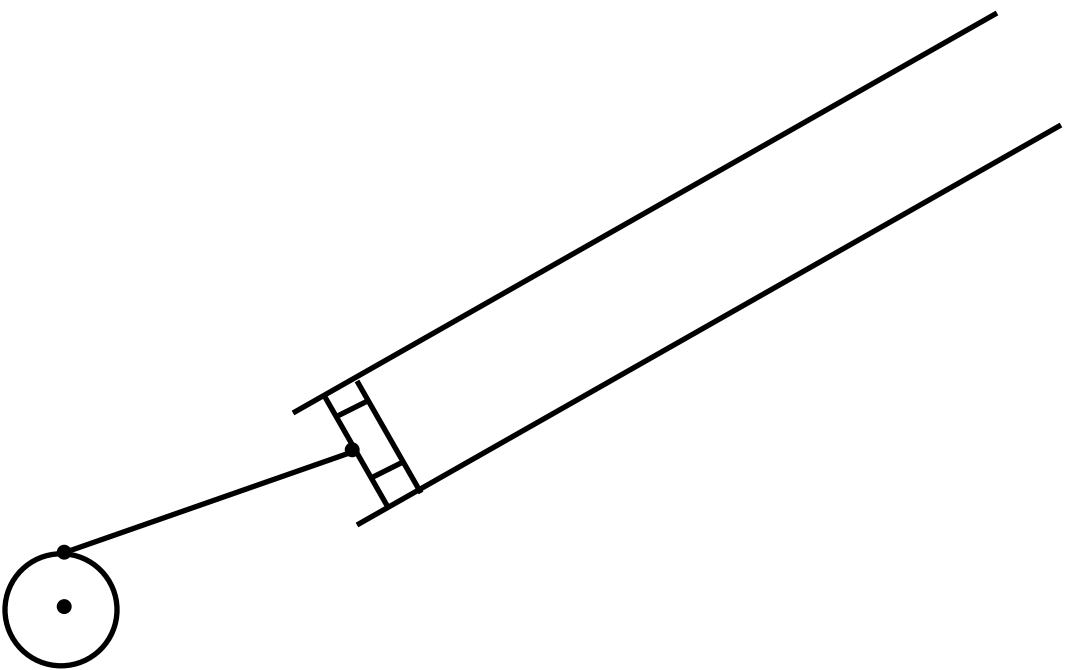
$$v_{\text{max}} = \frac{P}{2}a$$



Reduction of the effective gravity  $g \cdot \cos \theta$  along inclined magnetic flux tubes:

- ⇒ increasing of the acoustic cutoff period  $P_{\text{ac}}$ , i.e., lowering of the cutoff frequency
- ⇒ propagation of p-modes into the chromosphere as N-shaped shocks
- ⇒ lift of the chromosphere-transition region interface seen as a fibril

# N-shaped magnetoacoustic shocks



acoustic cutoff period

$$P_{\text{ac}} = \frac{4\pi}{g \cos \theta} \sqrt{\frac{RT}{\gamma \mu}}$$

$$E_{\text{kin}} = \frac{1}{2} \rho v^2 = \text{const.}$$

from shock discontinuity to parabola

$$v = v_{\text{max}} - at$$

$$y = y_0 + v_{\text{max}}t - \frac{a}{2}t^2$$

$$v_{\text{max}} = \frac{P}{2}a$$

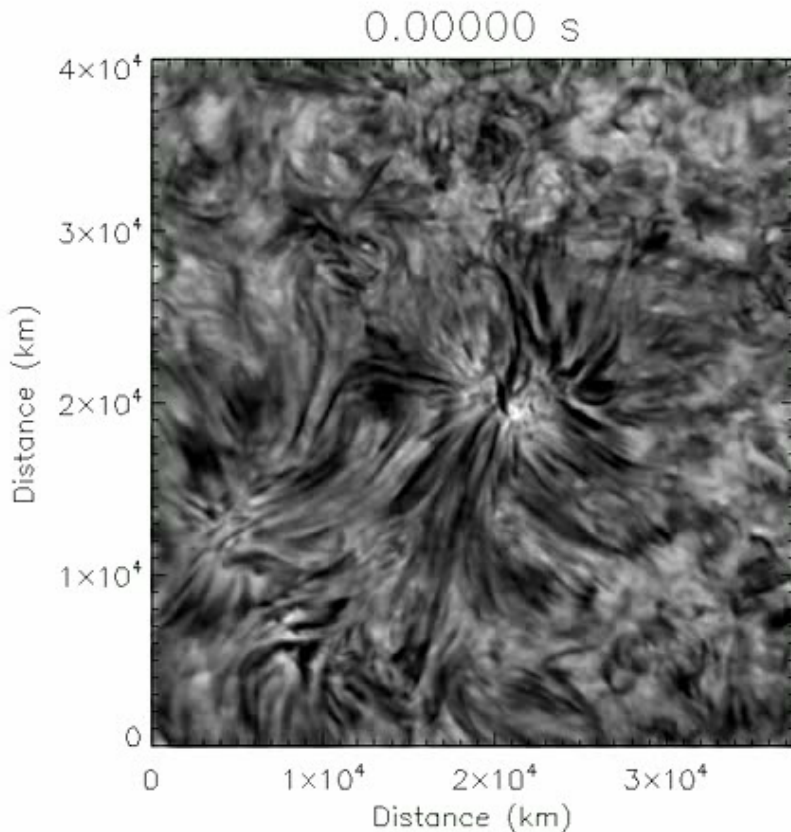
[Steiner 2012: IAUSS 6, 101](#)

What is this piston exactly?

Is it the 5-min oscillations?

Could it be a transversal movement of a flux tube with  
subsequent mode coupling to longitudinal waves?

# Kink waves of Type I spicules generated by photospheric pressure oscillations



Dunn Solar Telescope

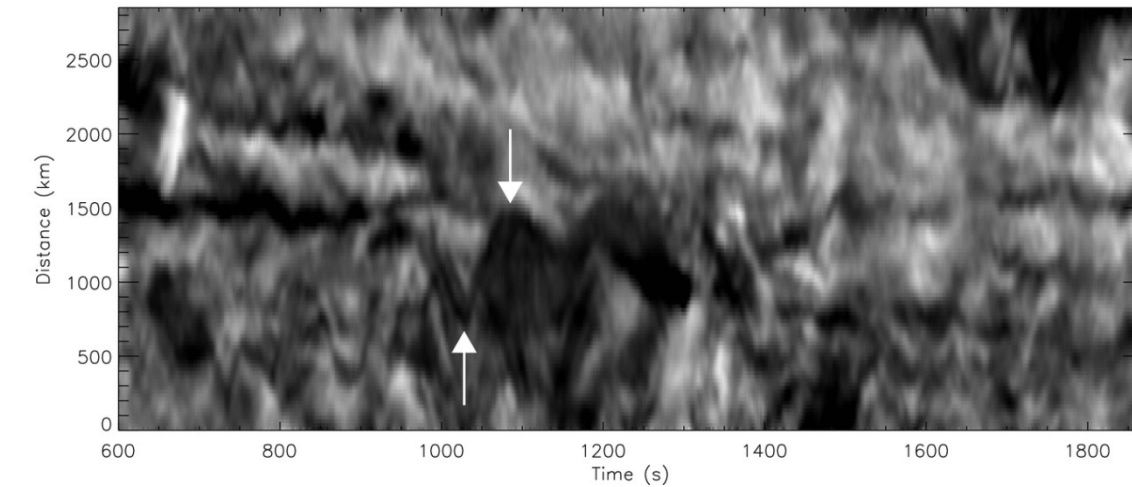
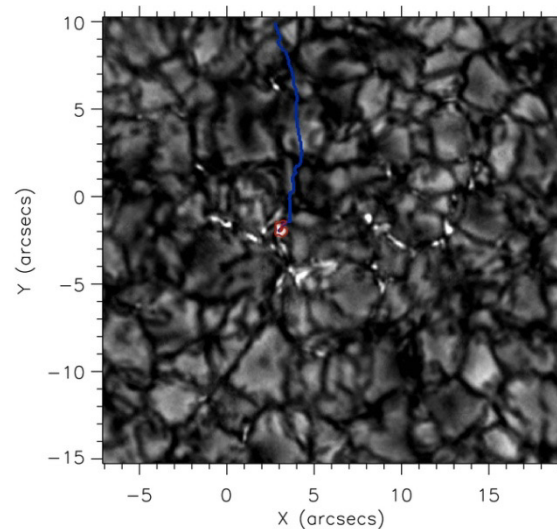
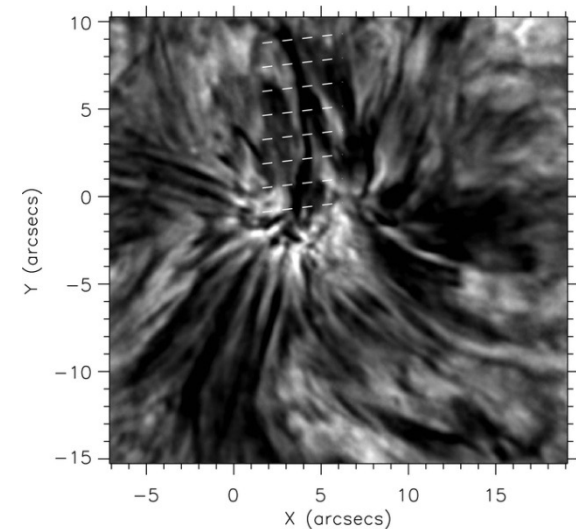
ROSA = Rapid Oscillations in  
the Solar Atmosphere

2009 May 28

H $\alpha$  cadence: 4.2 s  
G-band cadence: 0.53 s

[Jess et al. 2012: ApJL 744, 5](#)

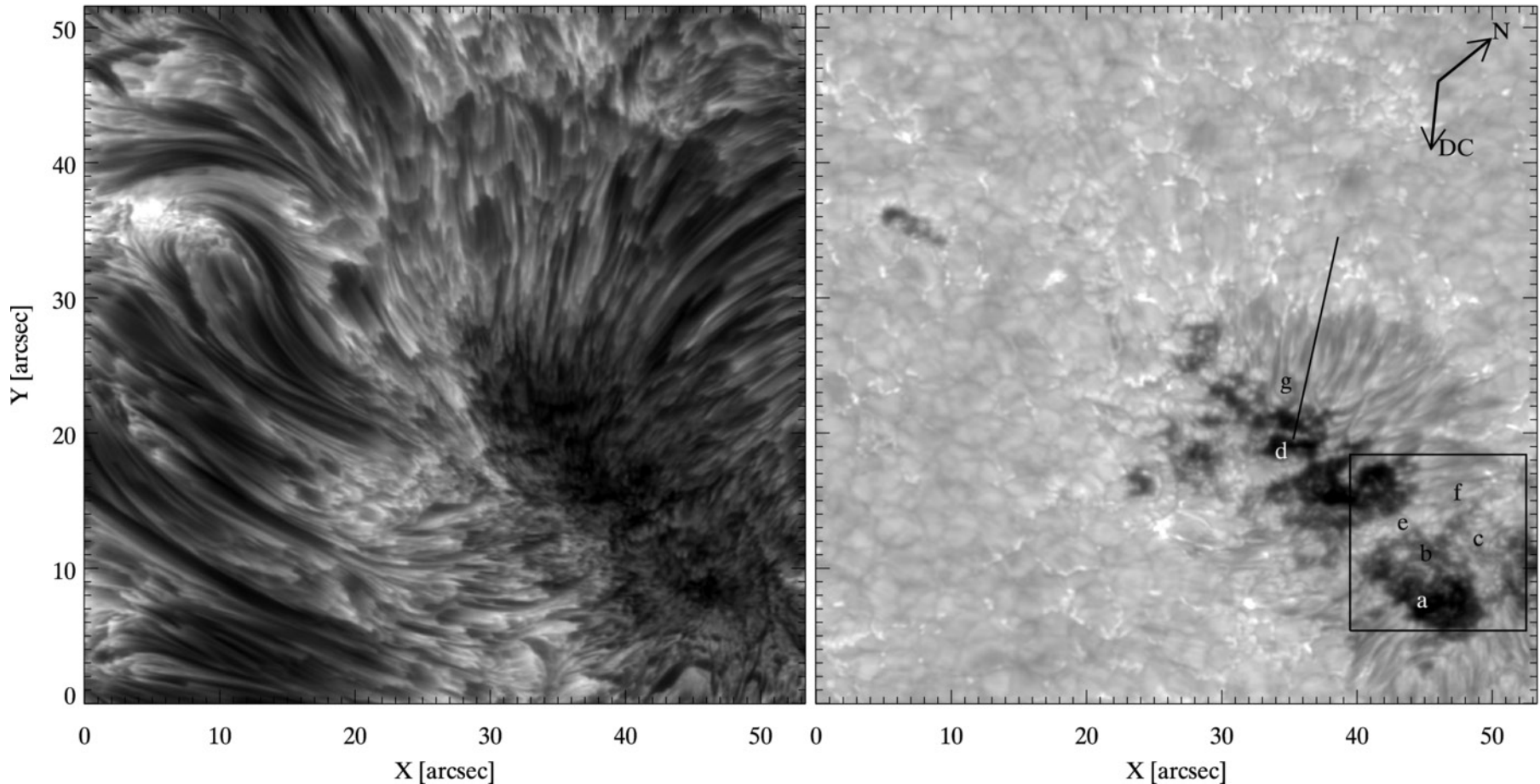
# Kink waves of Type I spicules generated by photospheric pressure oscillations



- intensity oscillations of photospheric magnetic bright points with periodicities of 130–440 s
- kink waves of Type I spicules with periodicities of 65–220 s
- longitudinal-to-transverse mode conversion into waves at half the initial driving period

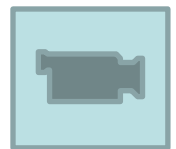
[Jess et al. 2012: ApJL 744, 5](#)

# Short dynamic fibrils in the sunspot chromosphere

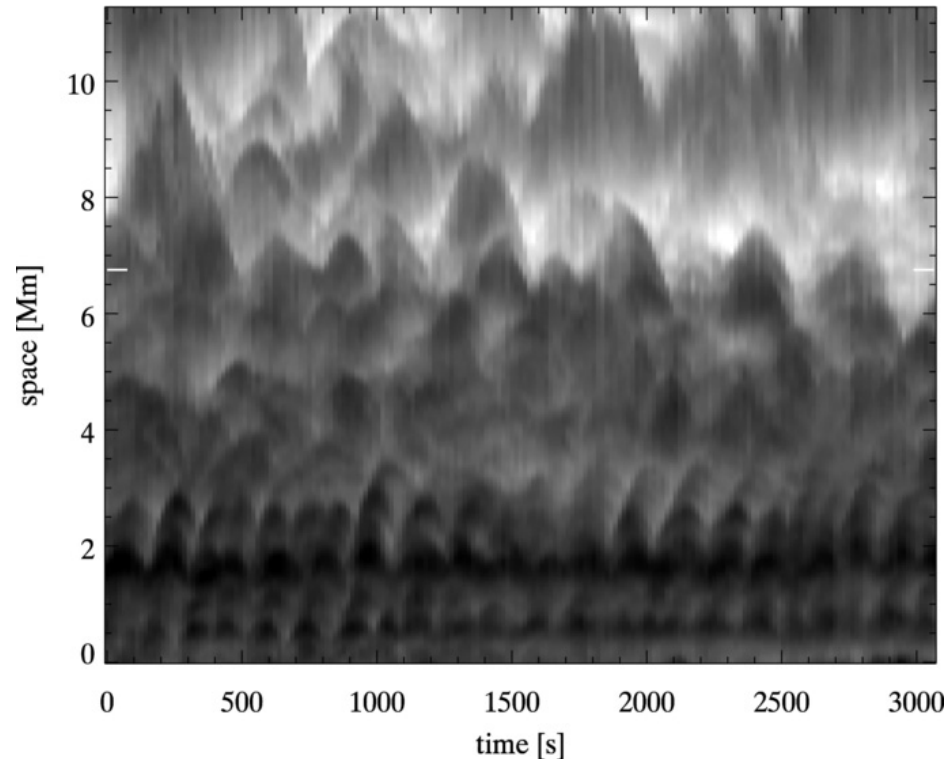


CRISP / SST    2011 May 4

[Rouppe van der Voort & de la Cruz Rodríguez 2013: ApJ 776, 56](#)

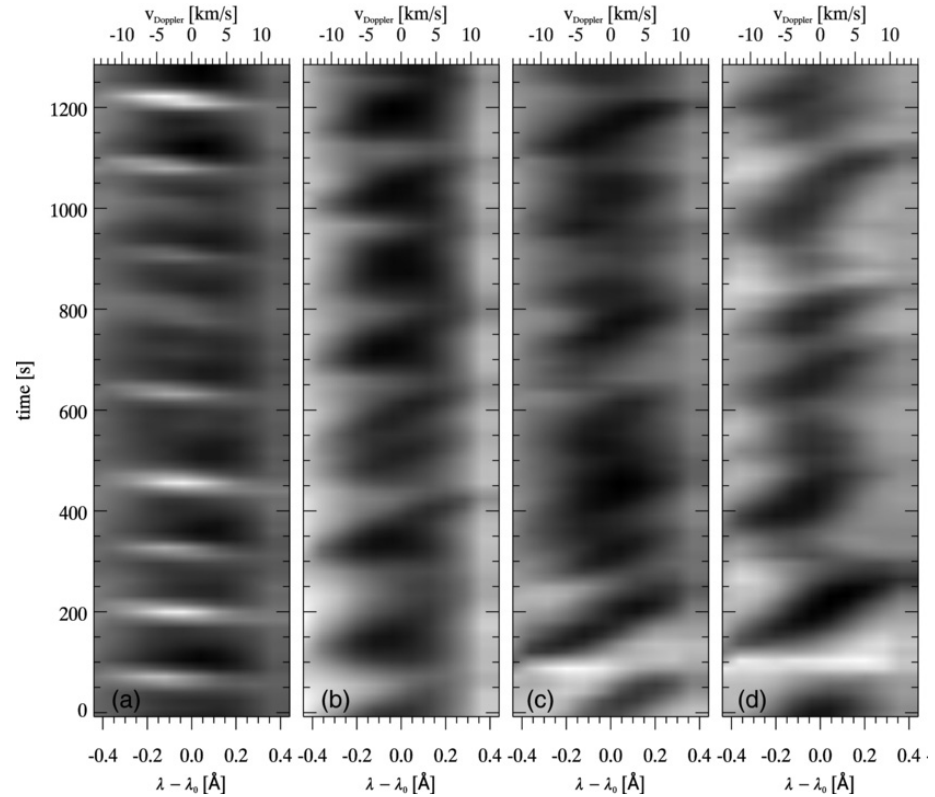


# Short dynamic fibrils in the sunspot chromosphere



*x-t* diagram

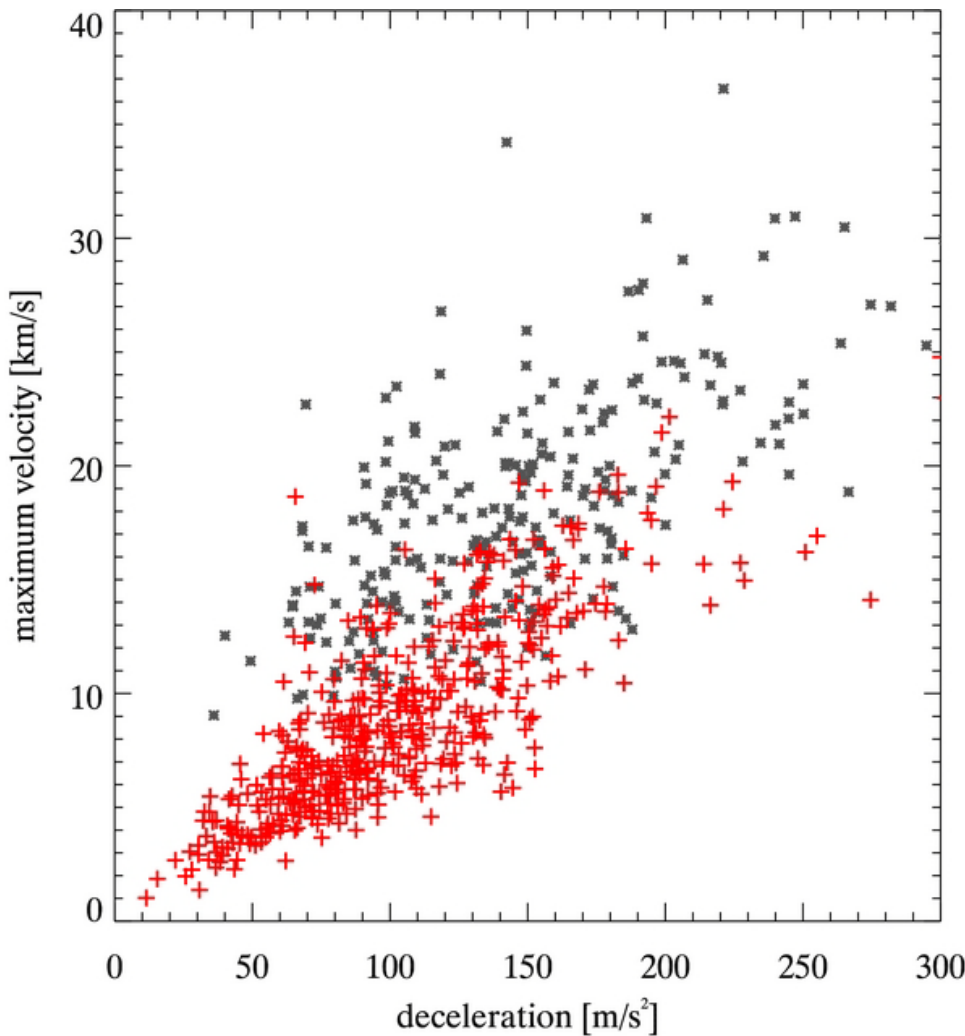
Parabolic top trajectories of dynamic fibrils in the sunspot.



*λ-t* diagram

Extensions and retractions of dynamic fibrils are actual mass motions.

# Short dynamic fibrils in the sunspot chromosphere



Maximum velocity  
versus  
deceleration

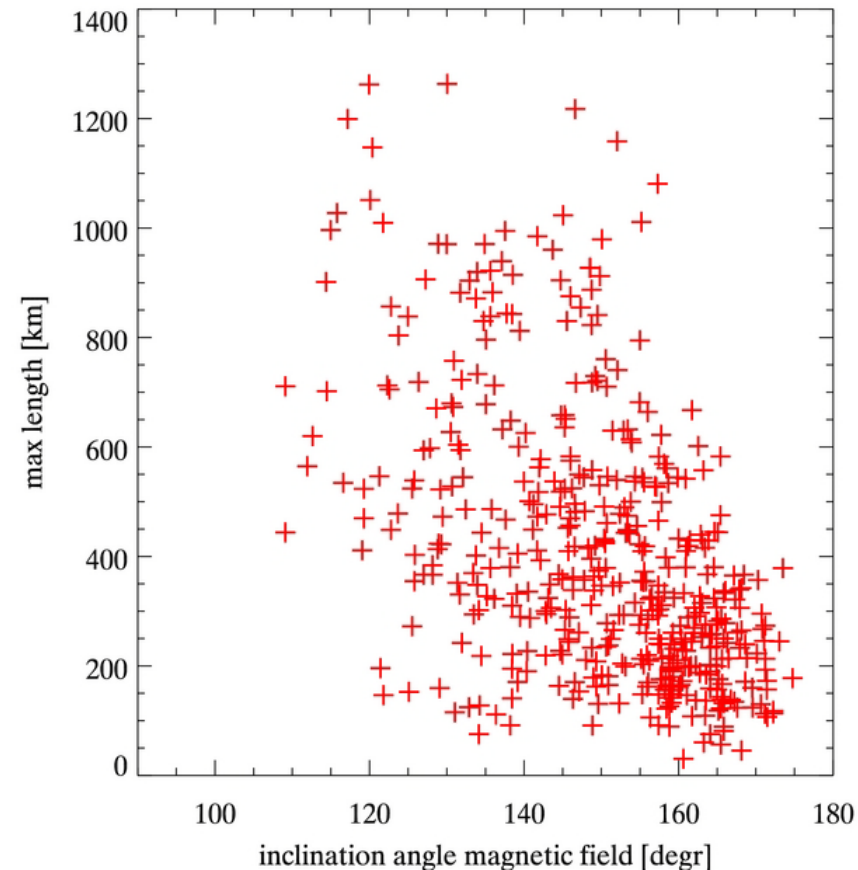
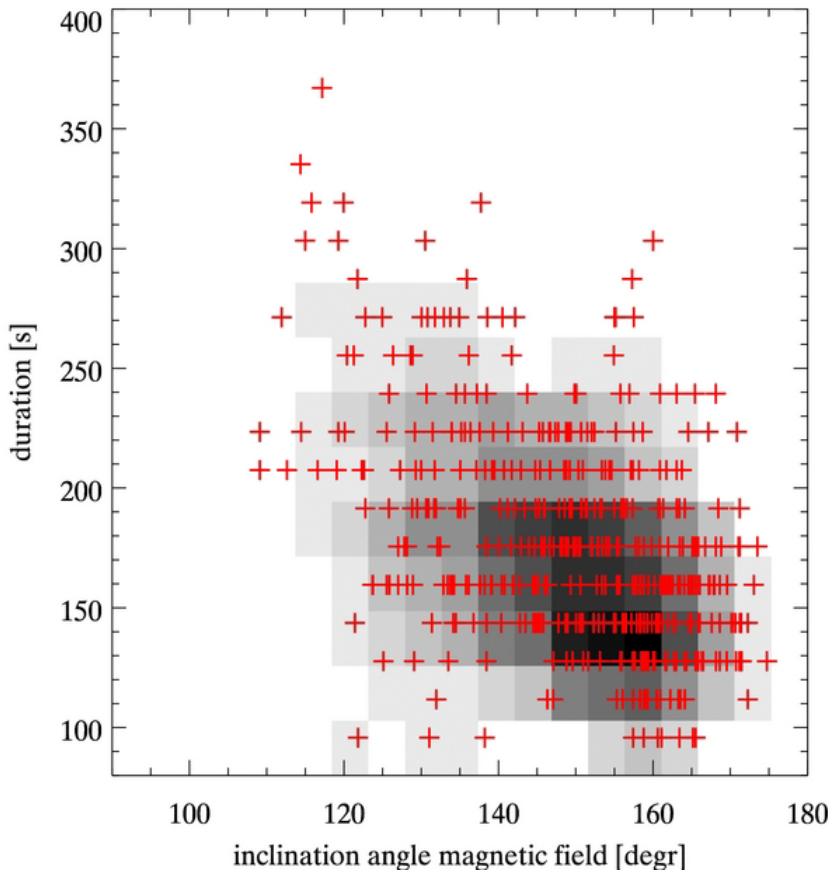
\* dynamic fibrils in plage

+ dynamic fibrils in sunspot

Indication of a common shock driver

# Short dynamic fibrils in the sunspot chromosphere

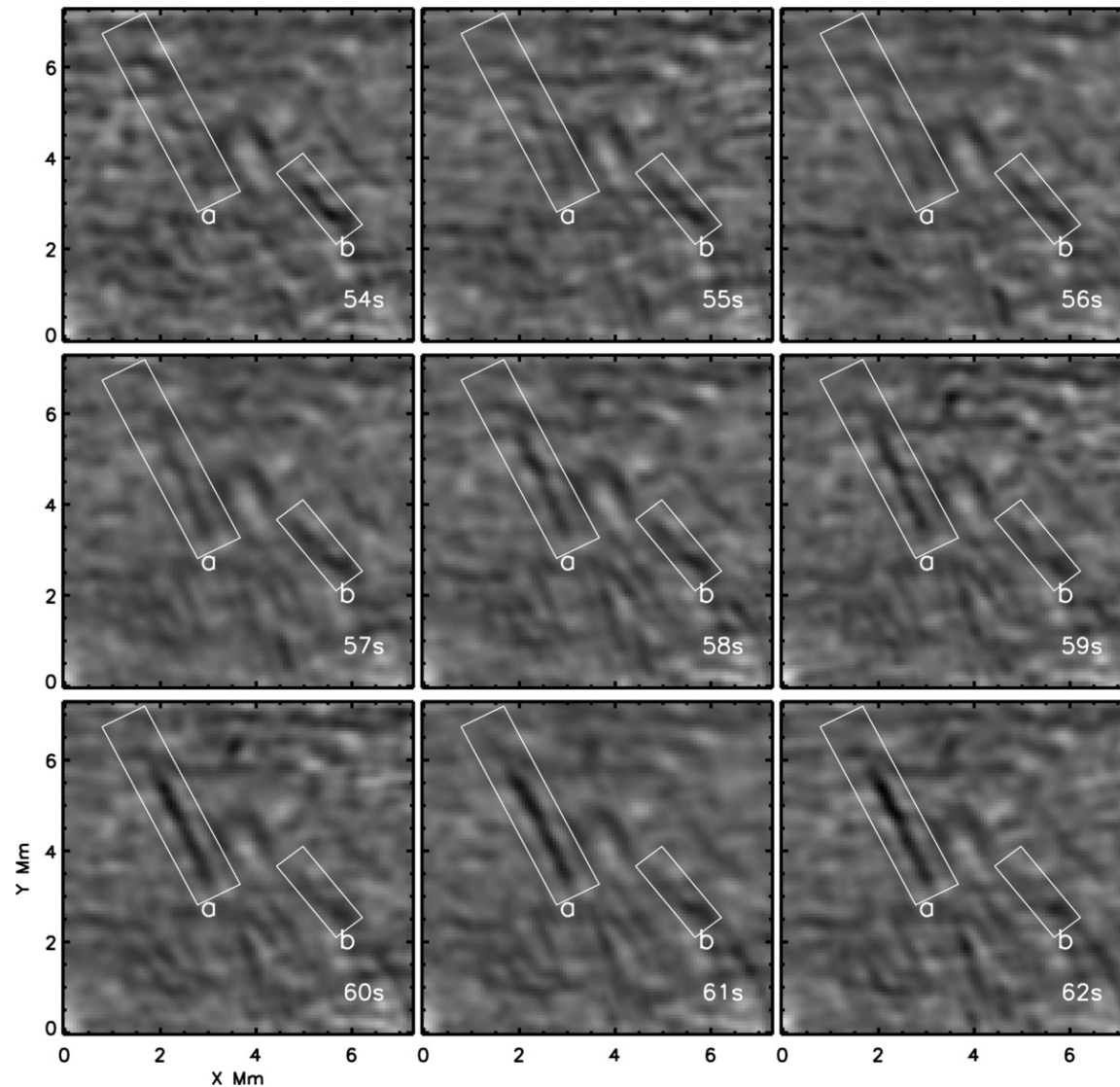
Relation between magnetic field inclination and dynamic fibril duration and length.



Inclination angle from an LTE inversion of Ca II 8542 Å

[Rouppe van der Voort & de la Cruz Rodríguez 2013: ApJ 776, 56](#)

# Evidence for sheet-like elementary structures in the sun's atmosphere?



Chromospheric fine structures =  
“striations of curtains blowing in  
the wind.”



A 9-s long IBIS sequence in the  
red wing of H $\alpha$  observed with  
1-s cadence.

Region (a) shows the  
appearance and region (b) the  
disappearance of dark features  
over several Mm in a few  
seconds.

# Magnetic field in spicules

## Spectropolarimetry

Trujillo Bueno et al. 2005: ApJ 619, 191

≈ 10 G at height 2000 km, inclination ≈ 35°, He I 10830 Å, VTT / TIP

López Ariste & Casini 2005: A&A 436, 325

10 – 30 G, He I 10830 Å, DST / ASP

Centeno et al. 2010: ApJ 708, 1579

- magnetic field strength of 50 G in network spicules
- He I 10830 Å, VTT/TIP, Hanle and Zeeman effects, HAZEL inversion

Ramelli et al. 2005: ESASP 596, 82

Ramelli et al. 2011: ASPC 437, 109

≈ 10 – 40 G, He I 10830 Å, ZIMPOL, HAZEL inversion

# Magnetic field in spicules

## Spectropolarimetry

Trujillo Bueno et al. 2005: ApJ 619, 191

≈ 10 G at height 2000 km, inclination ≈ 35°, He I 10830 Å, VTT / TIP

López Ariste & Casini 2005: A&A 436, 325

10 – 30 G, He I 10830 Å, DST / ASP

Centeno et al. 2010: ApJ 708, 1579

- the magnetic field strength of 50 G in network spicules
- He I 10830 Å, VTT/TIP, Hanle and Zeeman effects, HAZEL inversion

Ramelli et al. 2005: ESASP 596, 82

Ramelli et al. 2011: ASPC 437, 109

≈ 10 – 40 G, He I 10830 Å, ZIMPOL, HAZEL inversion

## Magnetoseismology

Zaqarashvili et al. 2007: A&A 474, 627

- spectroscopy of spicules in H $\alpha$  at Abastumani Observatory
- the magnetic field strength of 12-15 G in spicules at the height of 6000 km above the photosphere

Kim et al. 2008: JKAS 41, 173

- kink waves in spicules, SOT / Hinode, Ca II H
- lower limit: 10 – 18 G, upper limit: 43 – 76 G

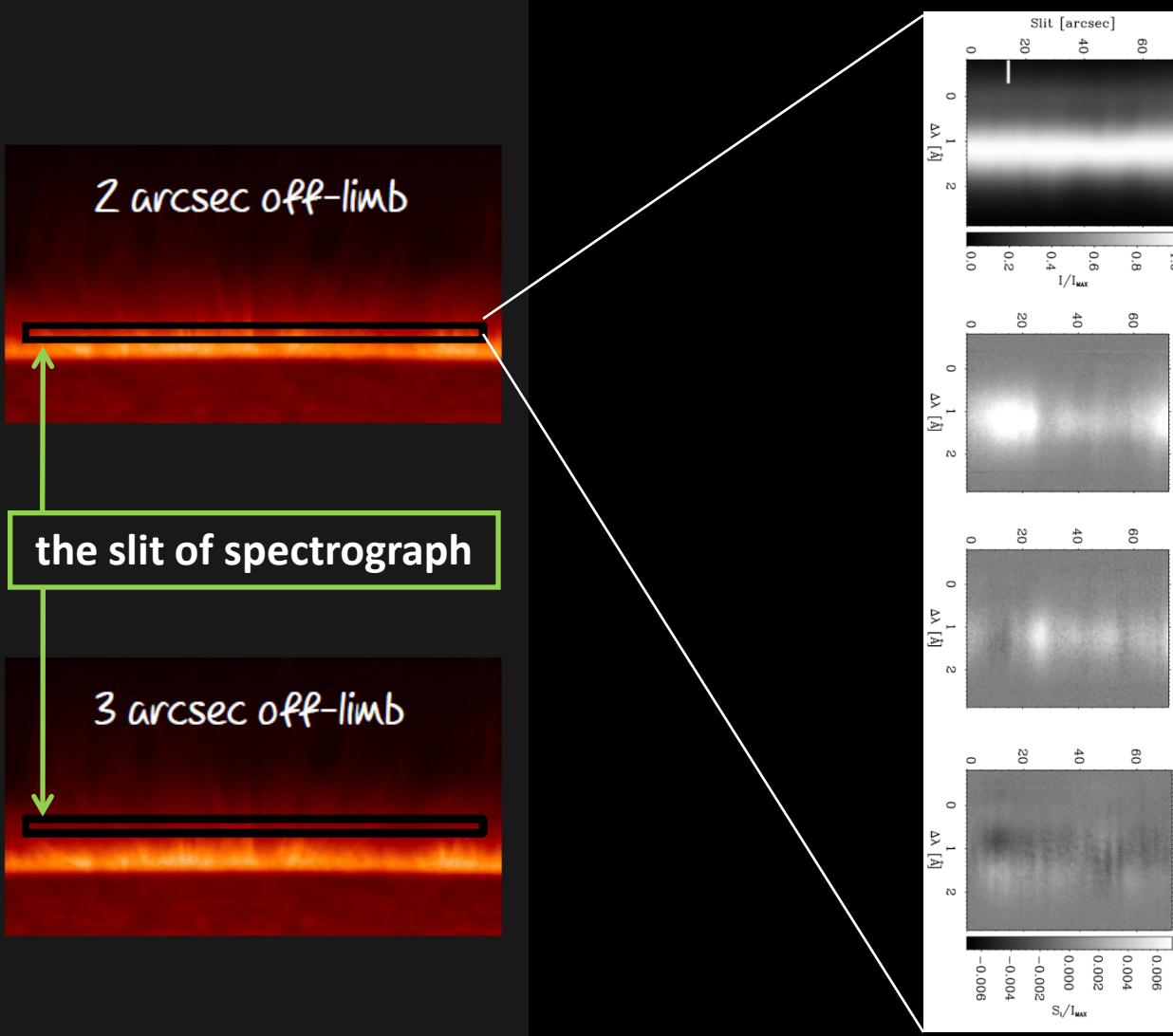
Verth et al. 2011: ApJL 733, 15

Pietarila et al. 2011: ApJ 739, 92

Kuridze et al. 2013: ApJ 779, 82

studies showing a decrease of normalized magnetic field strength with height in fibrils

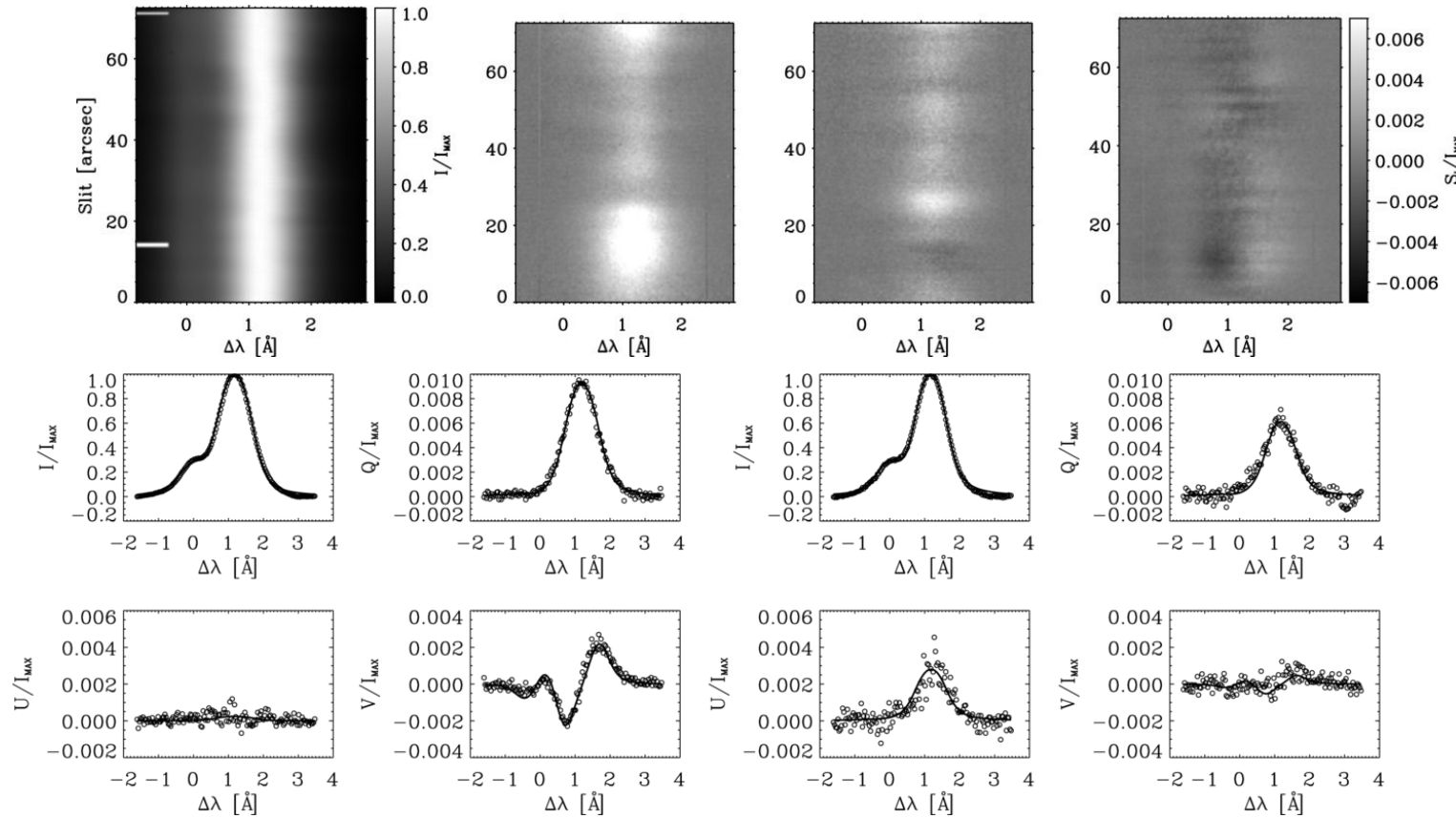
# Spectropolarimetry of spicules



German VTT + TIP  
He I 10 830 Å triplet  
17 August 2008

[Centeno et al. \(2008\)](#)

# The magnetic field of off-limb spicules



telescope + instrument:

German Vacuum Tower Telescope + TIP

date of obseravtion:

August 17, 2008

diagnostics:

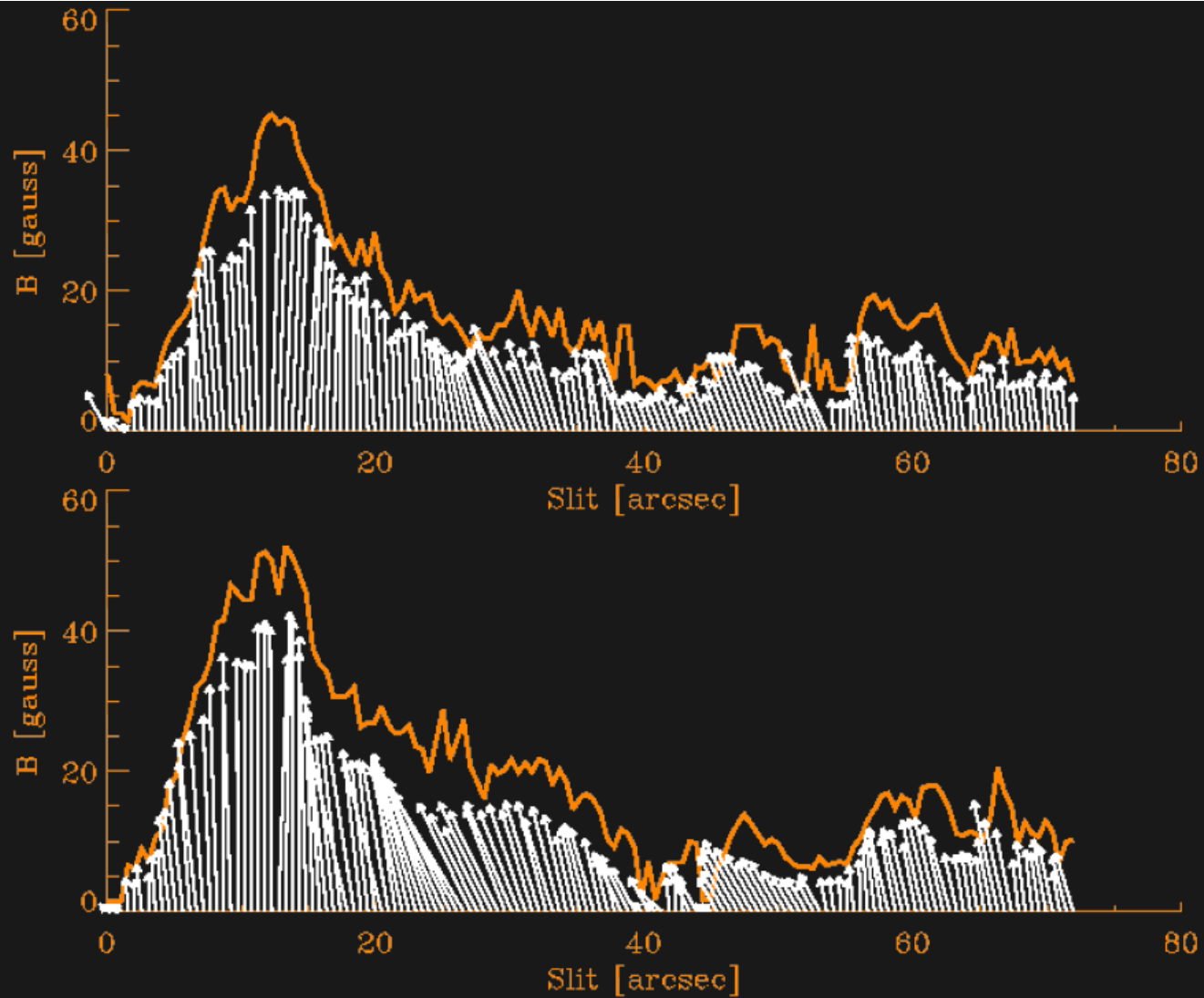
He I 10830 Å

## Main results:

- measurements of magnetic field strengths of spicules
- 48 G (left panels), 9 G (right panels)

# The magnetic field of off-limb spicules

2 arcsec off-limb

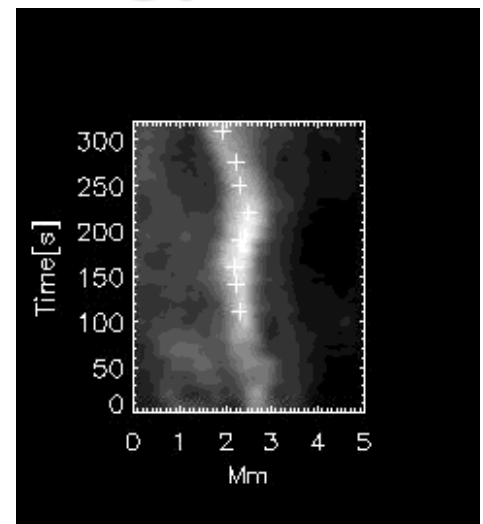
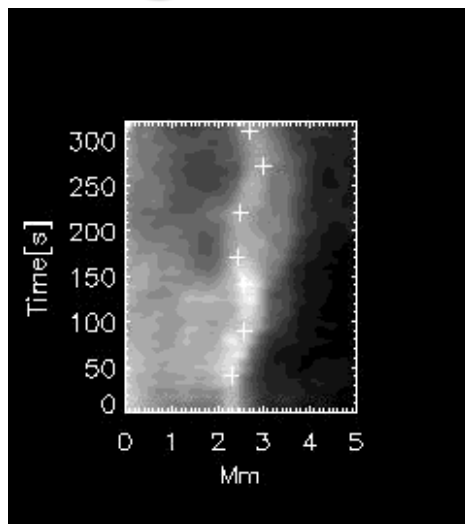
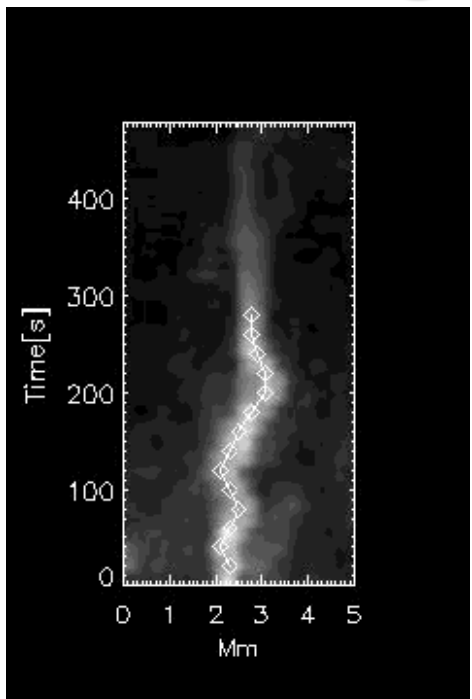


the slit of spectrograph

3 arcsec off-limb

[Centeno et al. \(2008\)](#)

# Estimation of the magnetic field in spicules using the magnetoseismology



Kink waves in spicules

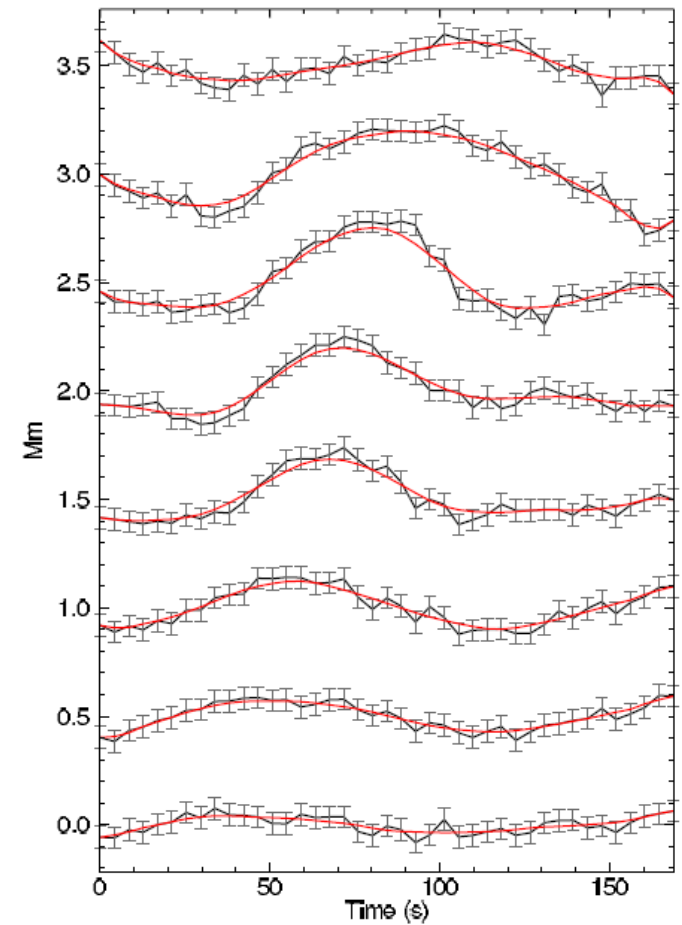
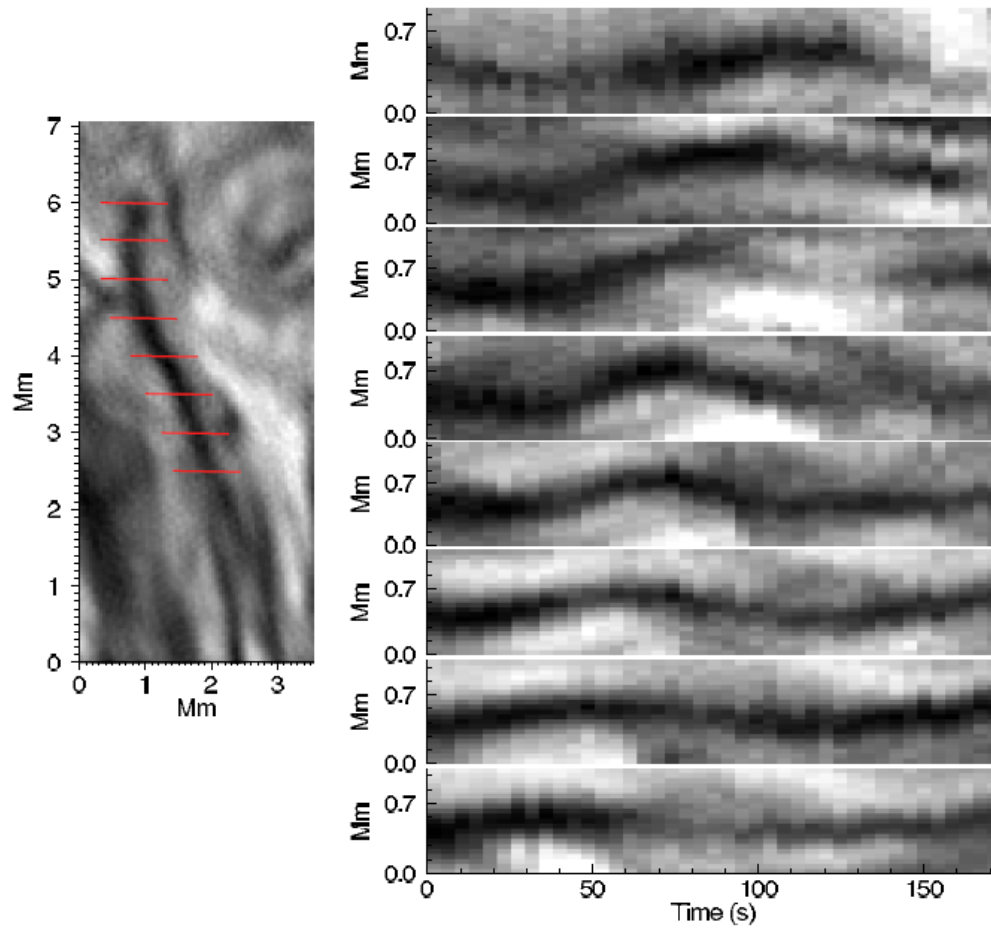
Ca II H, SOT / Hinode, 2008 June 3, 4

- lifetime of spicules: 5 – 7 min  
transverse displacements: 700 – 1000 km  
P – period of kink waves: 2 – 3 min  
L – min. wavelength: 45 000 – 60 000 km  
 $\rho_0, \rho_e$  – internal and external plasma density  
 $B_0$  – magnetic field strength:  
10 – 18 G for lower density limit  
43 – 76 G for upper density limit

[Kim et al. 2008: JKAS 41, 173](#)

$$B_0 = \sqrt{\frac{\mu_0}{2}} \frac{L}{P} \sqrt{\rho_0 \left(1 + \frac{\rho_e}{\rho_0}\right)},$$

# Transverse waves in chromospheric mottles



ROSA / DST    2009 May 28  
H $\alpha$  cadence: 4.2 s

[Kuridze et al. 2012: ApJ 750, 51](#)

[Kuridze et al. 2013: ApJ 779, 82](#)

# Transverse waves in chromospheric mottles

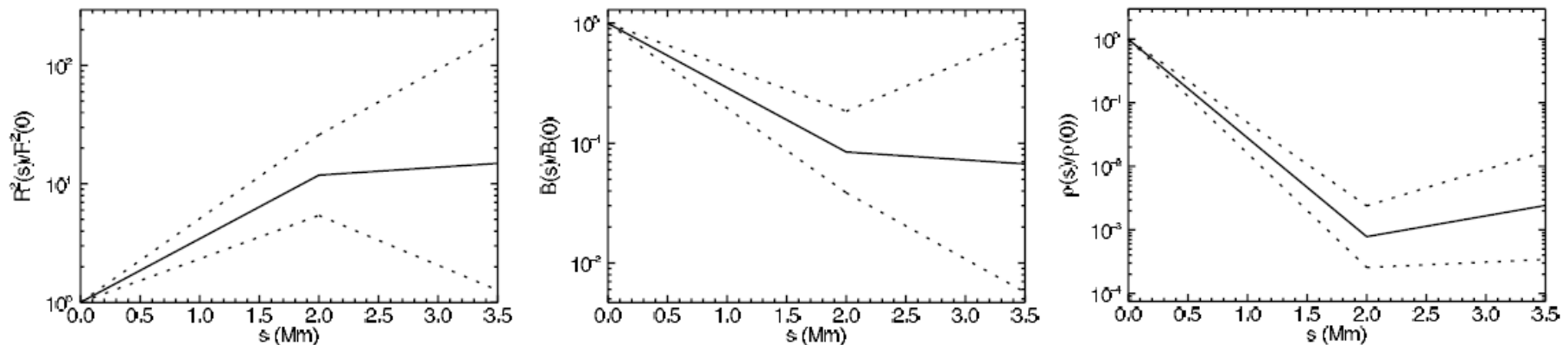


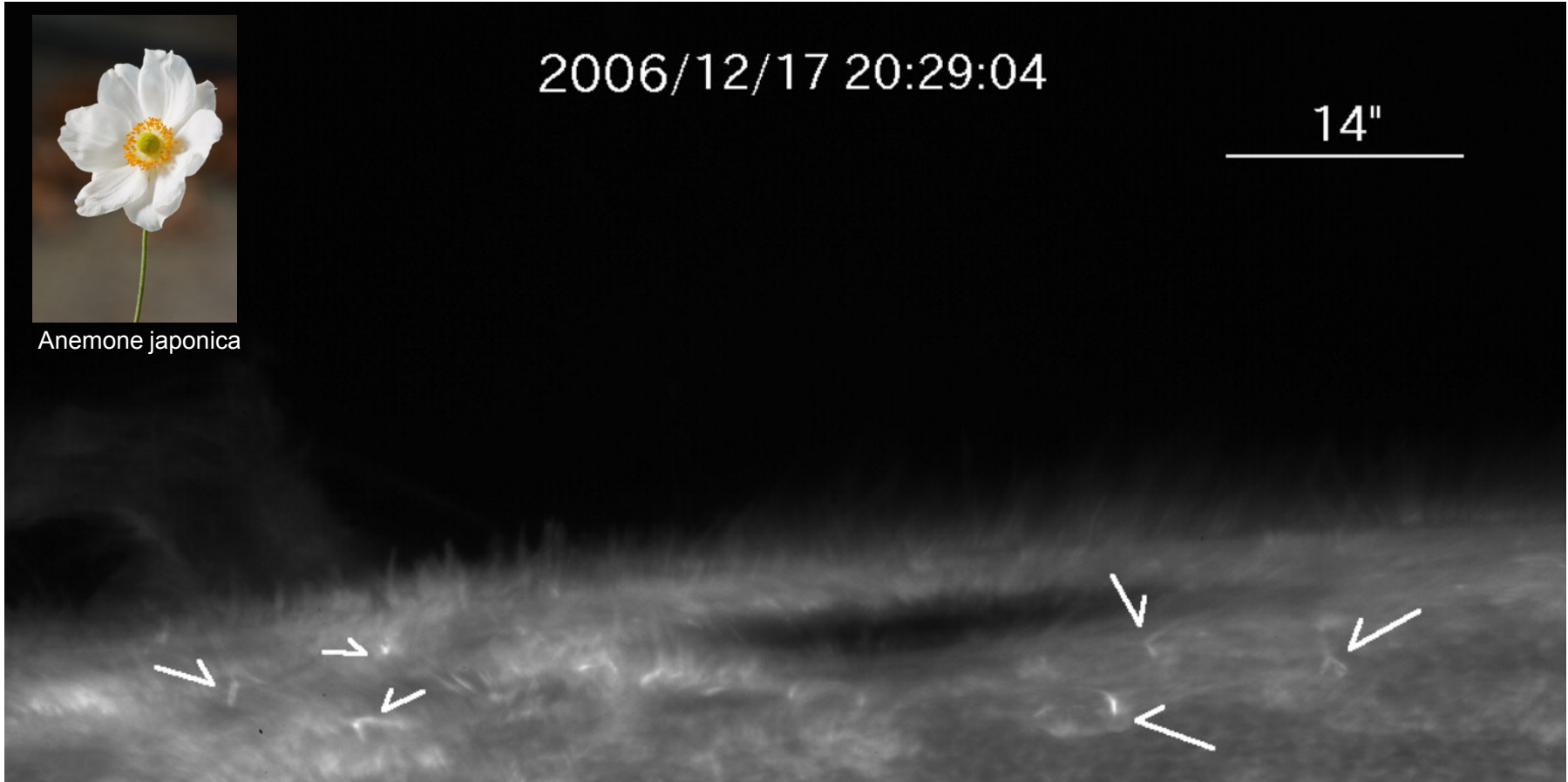
Figure 6. Normalized area expansion (left), magnetic field strength (middle), and plasma density (right), estimated using the techniques of magnetoseismology, plotted as a function of length along the waveguide shown in Figure 2. The dotted lines indicate the region of uncertainty due to the  $1\sigma$  error of  $A_1$  and  $A_2$ .

The magnetic field strength of the mottle along the  $\sim 2$  Mm length is found to decrease by a factor of 12, while the local plasma density scale height is  $\sim 280 \pm 80$  km.

[Kuridze et al. 2012: ApJ 750, 51](#)

[Kuridze et al. 2013: ApJ 779, 82](#)

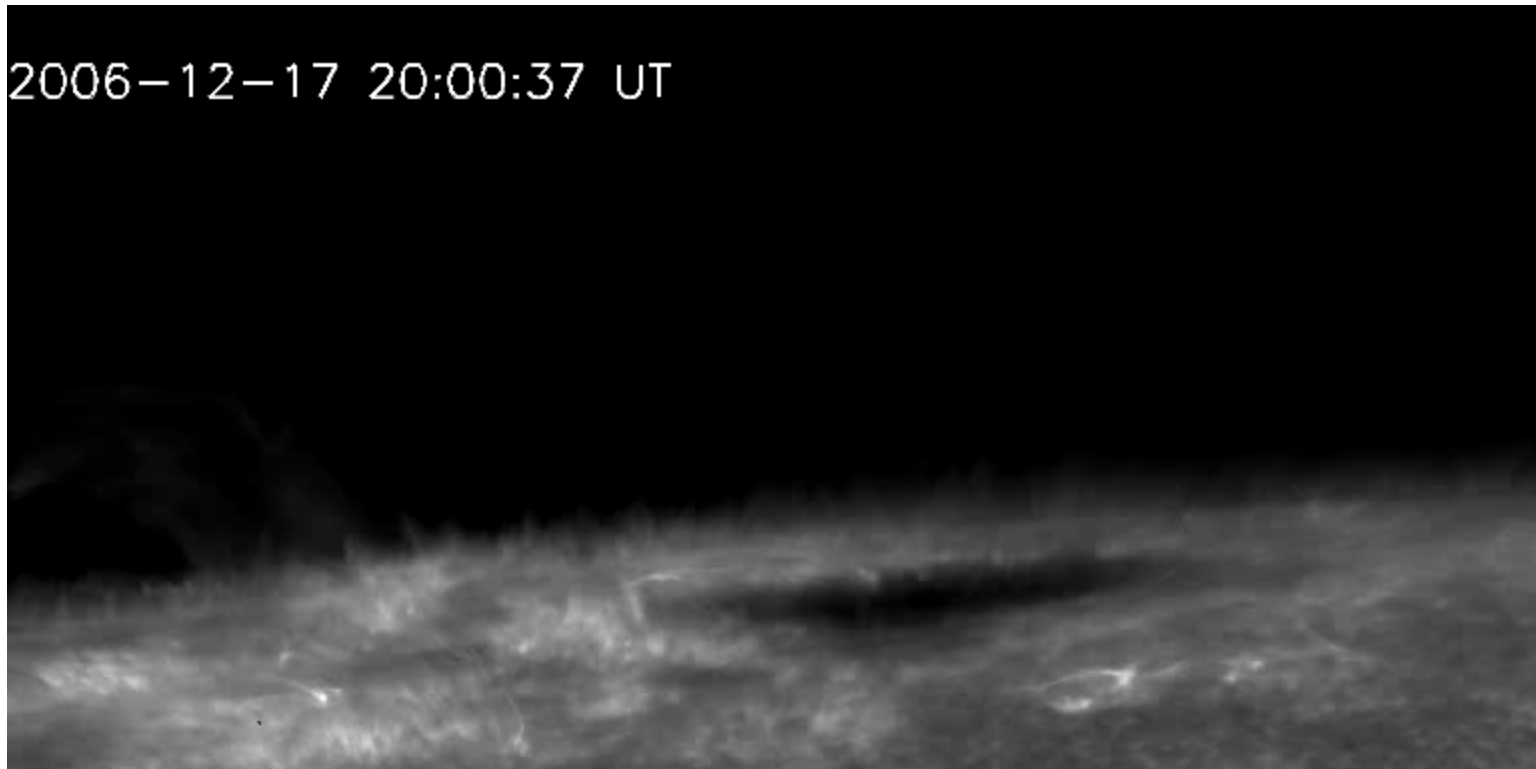
# Anemone jets in Ca II H by Hinode/SOT



[Shibata et al. 2007: Sci 318, 1591](#)

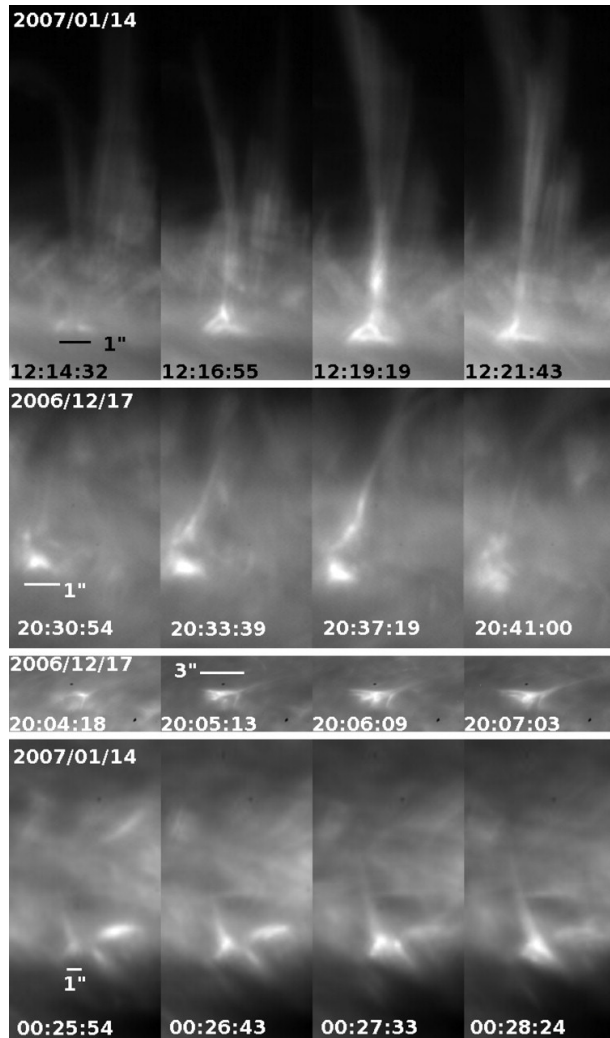
# Anemone jets in Ca II H by Hinode/SOT

2006-12-17 20:00:37 UT

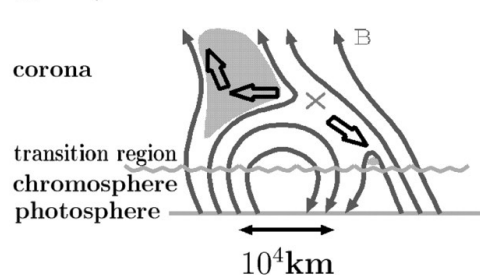


[Shibata et al. 2007: Sci 318, 1591](#)

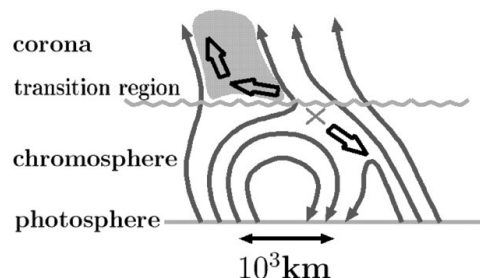
# Inverted Y-shape jets implying magnetic reconnection



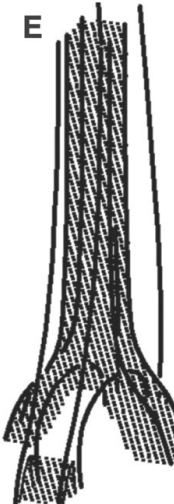
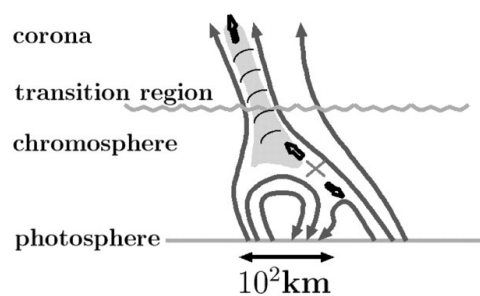
A X-ray Jets/SXR microflares



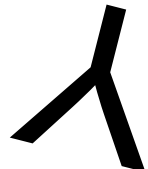
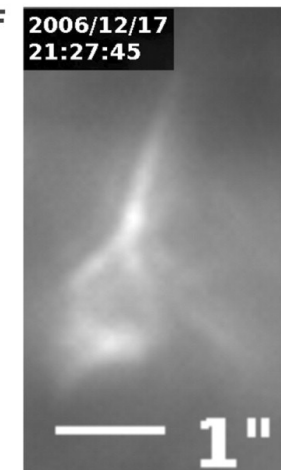
B EUV Jets/EUV microflares



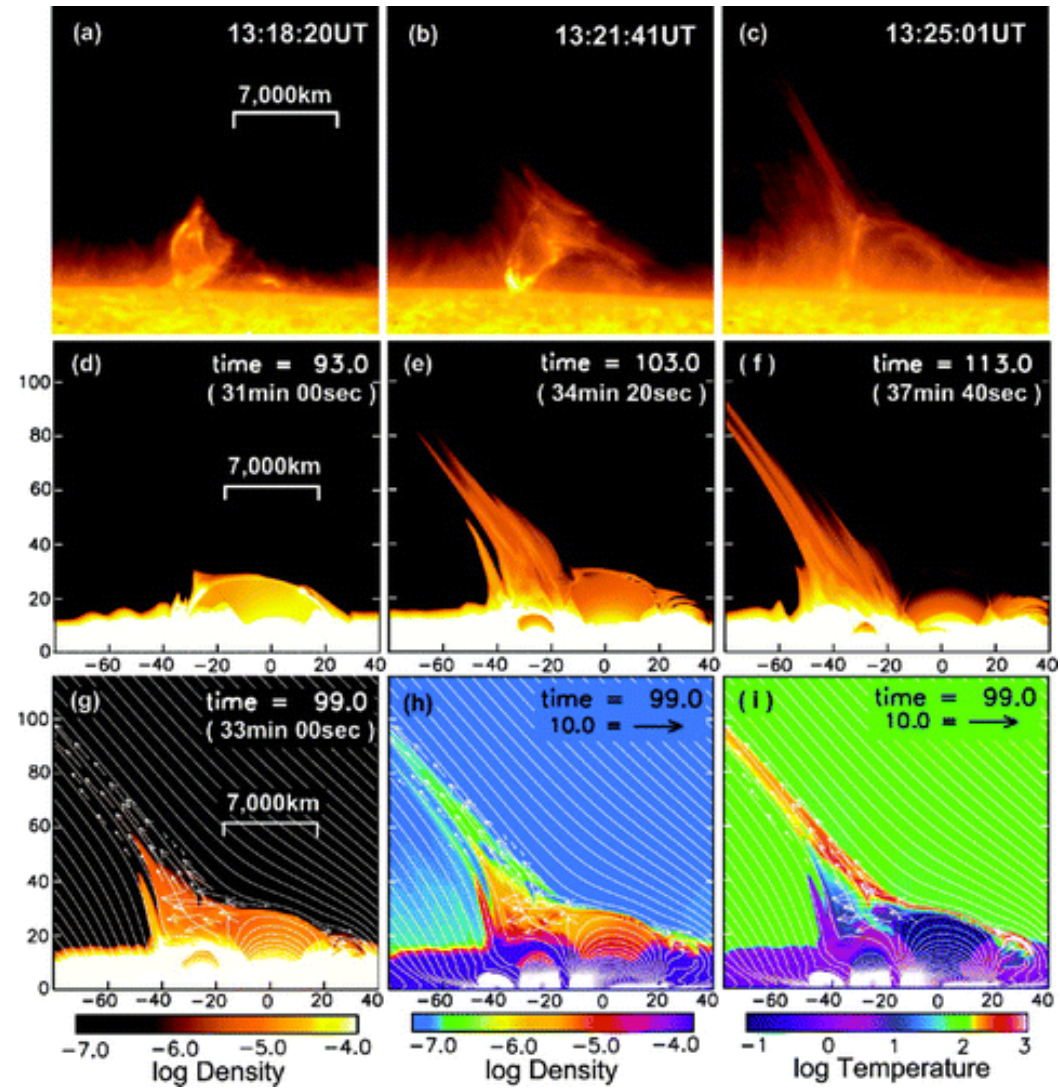
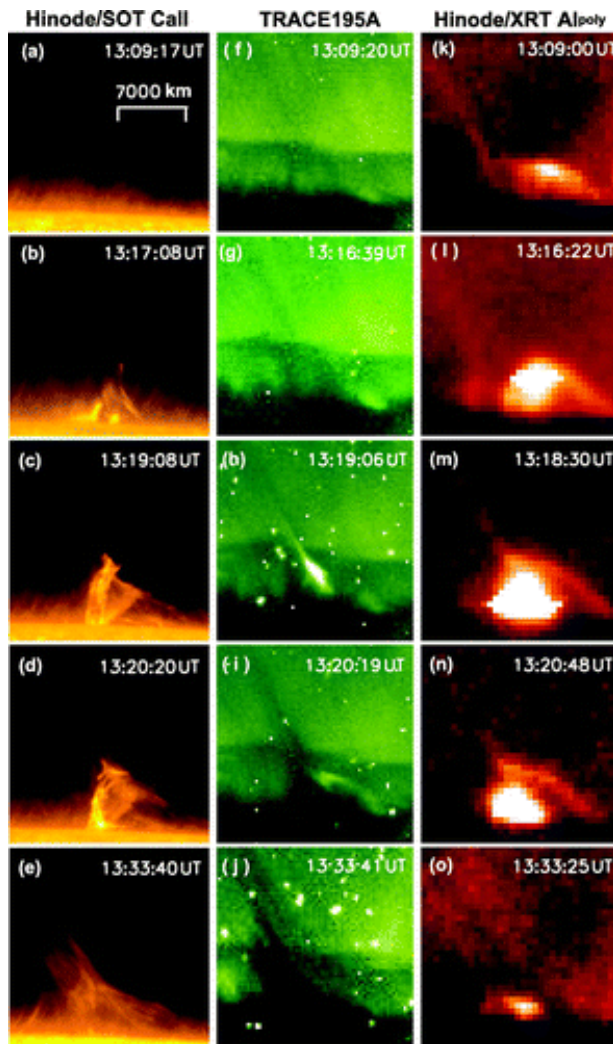
C Spicules Jets/Photospheric nanoflares (what?)



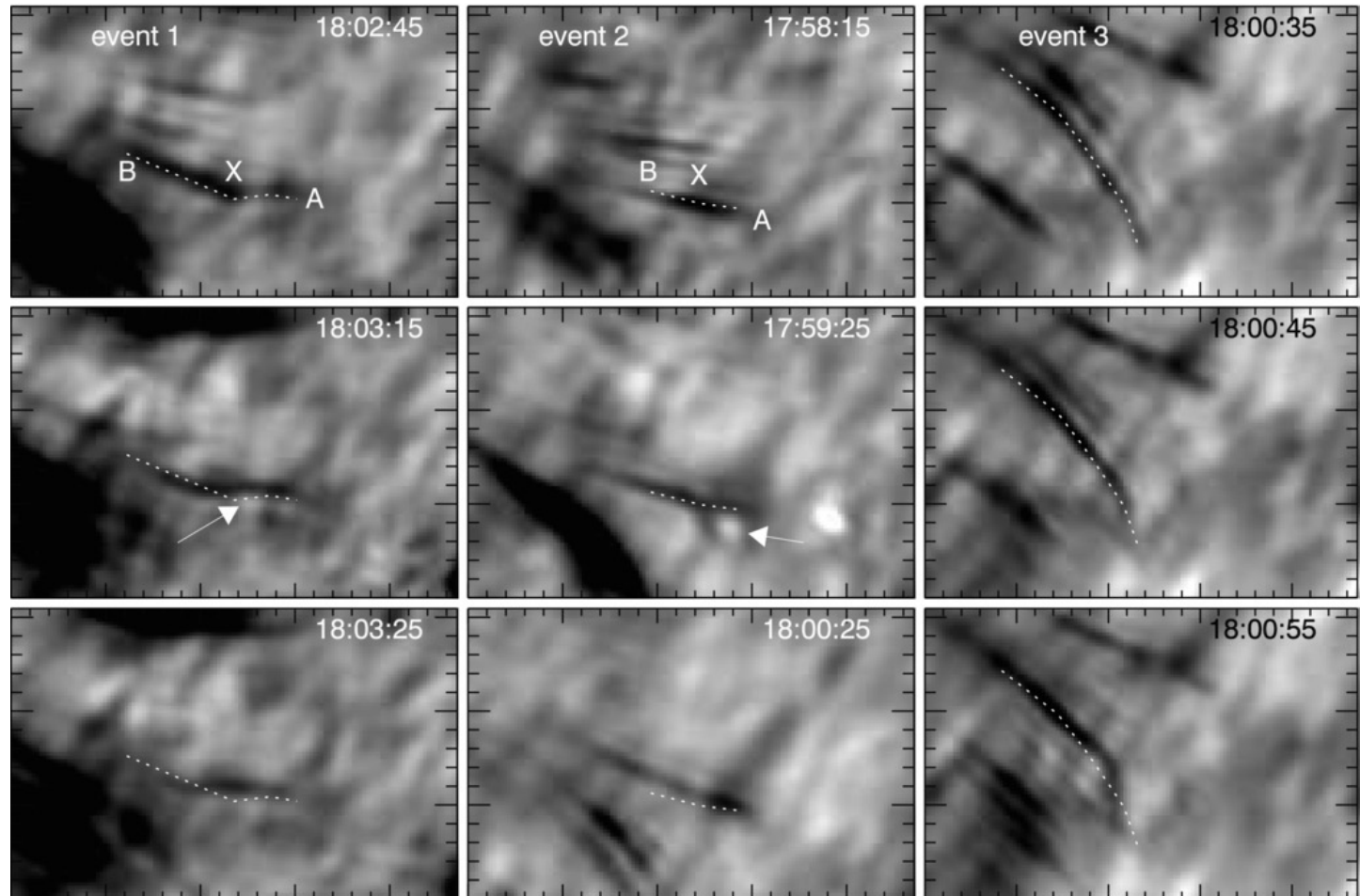
F 2006/12/17  
21:27:45



# Giant anemone jet in multispectral observations and simulations



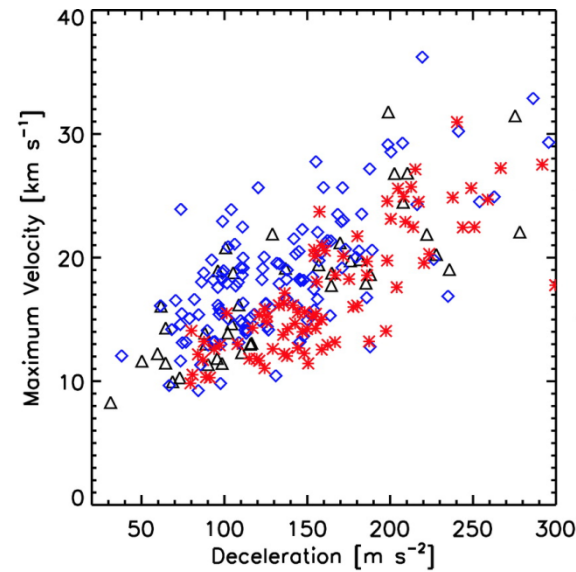
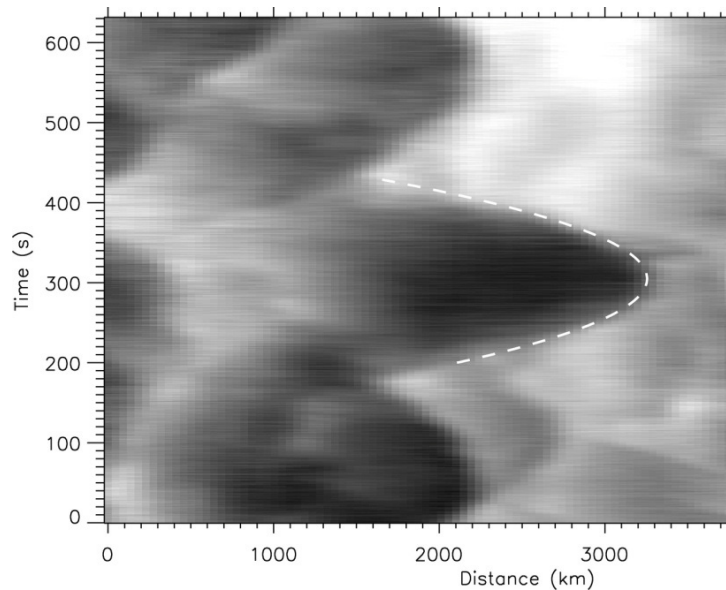
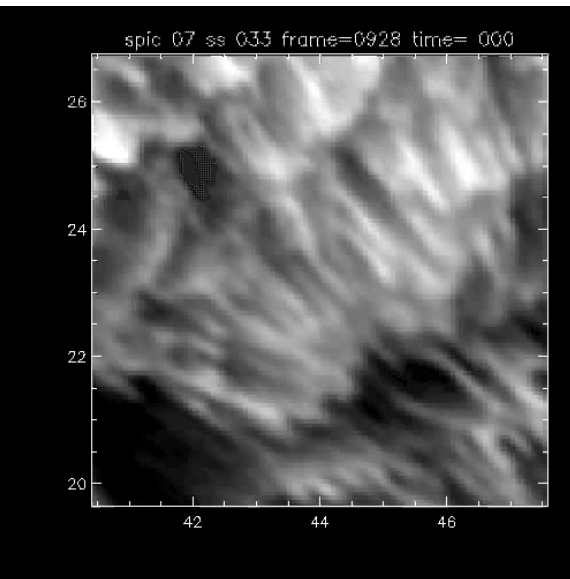
# Y-shaped rapid blueshifted excursions in the NST H $\alpha$ observations



H $\alpha$  at  $\Delta\lambda = -1 \text{ \AA}$

[Yurchyshyn et al. 2013: ApJ 767, 17](#)

# Dynamic fibrils in H $\alpha$



[Hansteen et al. 2006: ApJ 647, 73](#)

[De Pontieu et al. 2007: ApJ 655, 624](#)

## Main results:

- confirmed extensions and retractions
- confirmed parabolic top trajectories
- linear relationship between maximum velocity and deceleration
- H $\alpha$  dynamic fibrils in a plage co-spatial with areas of increased power of 5-min oscillations
- field-aligned magnetoacoustic shock excitation

# Numerical 1-D simulations of shock wave-driven chromospheric jets

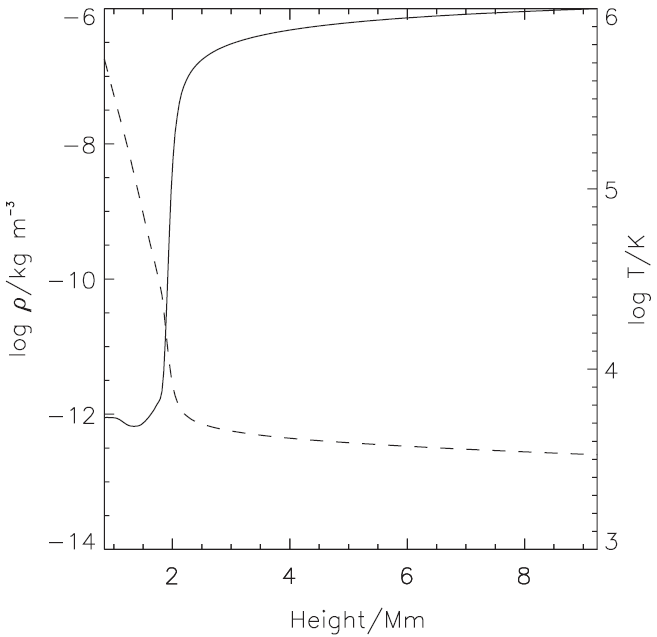
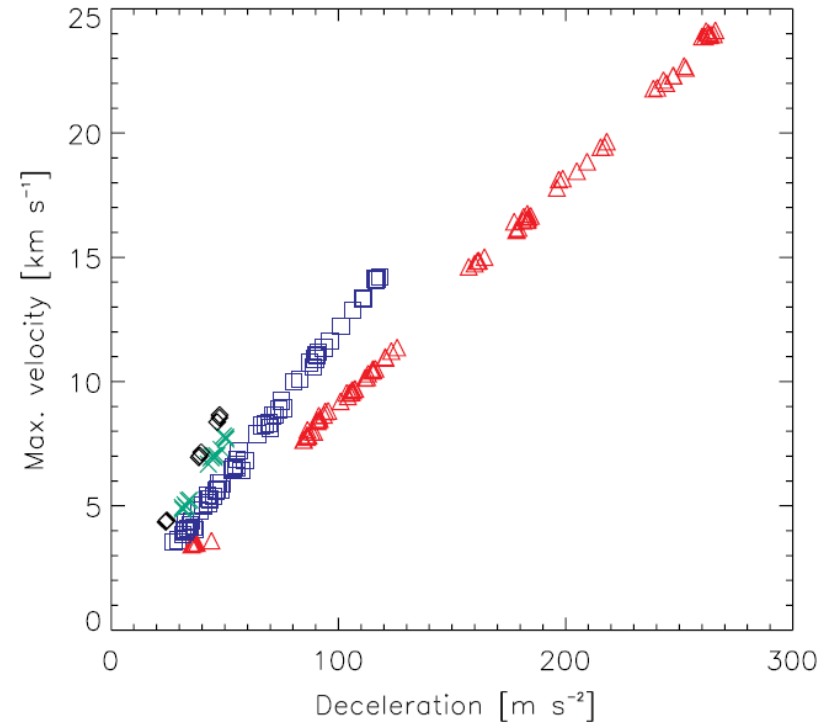
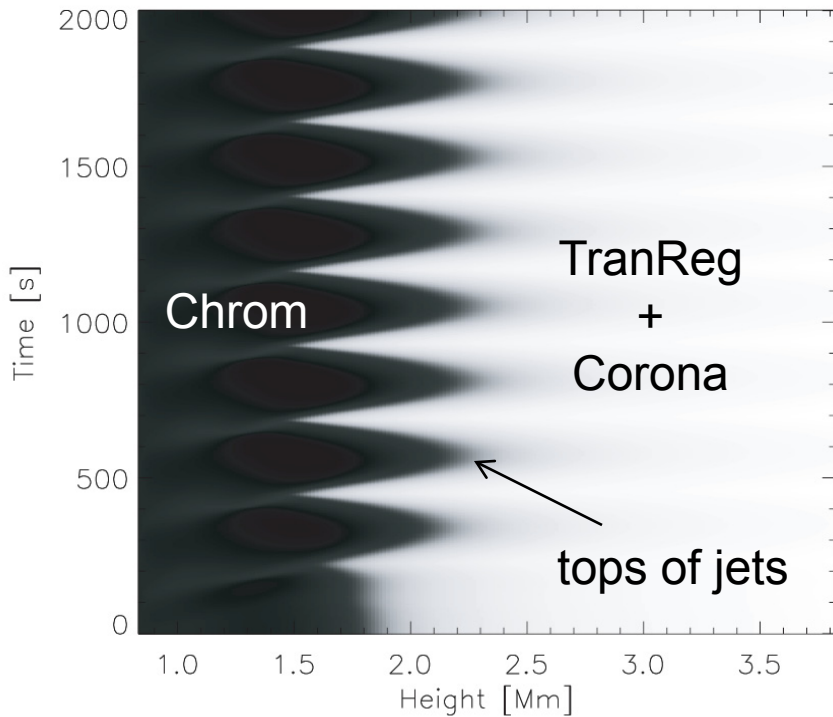


Fig. 1.—Initial density (dashed line, left axis) and temperature (solid line, right axis) structure of the model.

$$\begin{aligned}
 \frac{\partial \varrho}{\partial t} + \nabla \cdot (\varrho \mathbf{v}) &= 0, \\
 \frac{\partial \varrho \mathbf{v}}{\partial t} + \nabla \cdot \left[ \varrho \mathbf{v} \otimes \mathbf{v} + p_{\text{tot}} \underline{\underline{1}} - \frac{\mathbf{B} \otimes \mathbf{B}}{4\pi} \right] &= \varrho \mathbf{g} + \nabla \cdot \underline{\underline{\tau}}, \\
 \frac{\partial e}{\partial t} + \nabla \cdot \left[ \mathbf{v}(e + p_{\text{tot}}) - \frac{1}{4\pi} \mathbf{B}(\mathbf{v} \cdot \mathbf{B}) \right] &= \varrho(\mathbf{g} \cdot \mathbf{v}) \\
 &\quad + Q_{\text{rad}} + \frac{1}{4\pi} \nabla \cdot (\mathbf{B} \times \eta \nabla \times \mathbf{B}) + \nabla \cdot (\mathbf{v} \cdot \underline{\underline{\tau}}) + \nabla \cdot (K \nabla T) \\
 \frac{\partial \mathbf{B}}{\partial t} + \nabla \cdot [\mathbf{v} \otimes \mathbf{B} - \mathbf{B} \otimes \mathbf{v}] &= -\nabla \times (\eta \nabla \times \mathbf{B}),
 \end{aligned}$$

- 1-D magnetohydrodynamics (MHD) simulations
- chosen magnetic field strength: 60 G ( $6 \times 10^{-3}$  T)
- chosen field inclinations:  $0^\circ, 30^\circ, 45^\circ, 60^\circ$
- chosen piston periods: 180 s, 240 s, 300 s, 360 s
- chosen initial amplitudes:  $200 \text{ ms}^{-1}, 500 \text{ ms}^{-1}, 800 \text{ ms}^{-1}, 1100 \text{ ms}^{-1}$

# Numerical simulations of shock wave-driven chromospheric jets

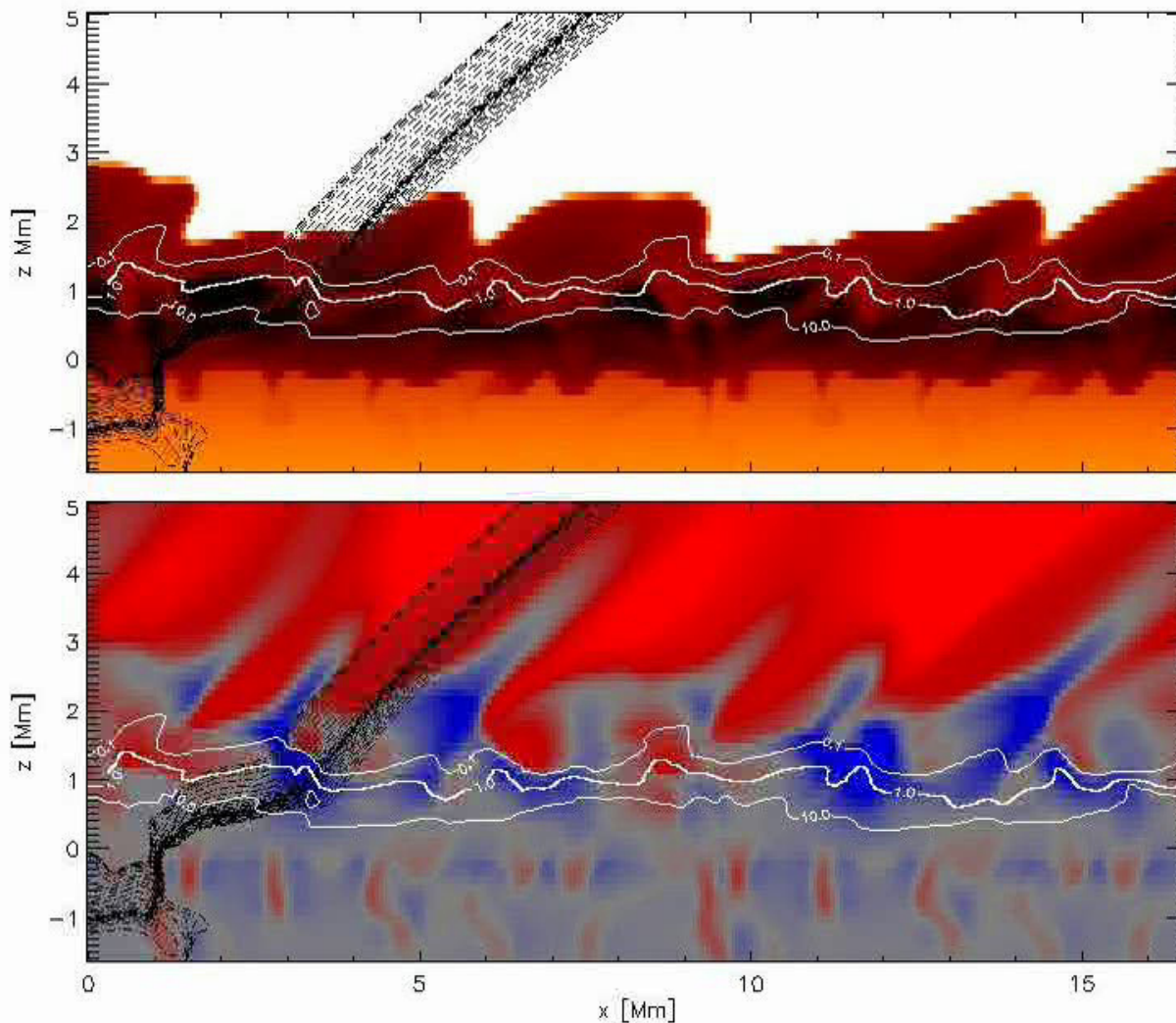


## Main results reproduce:

- parabolic shapes of Chrom – TranReg interface
- the range of observed decelerations and roughly max. velocities

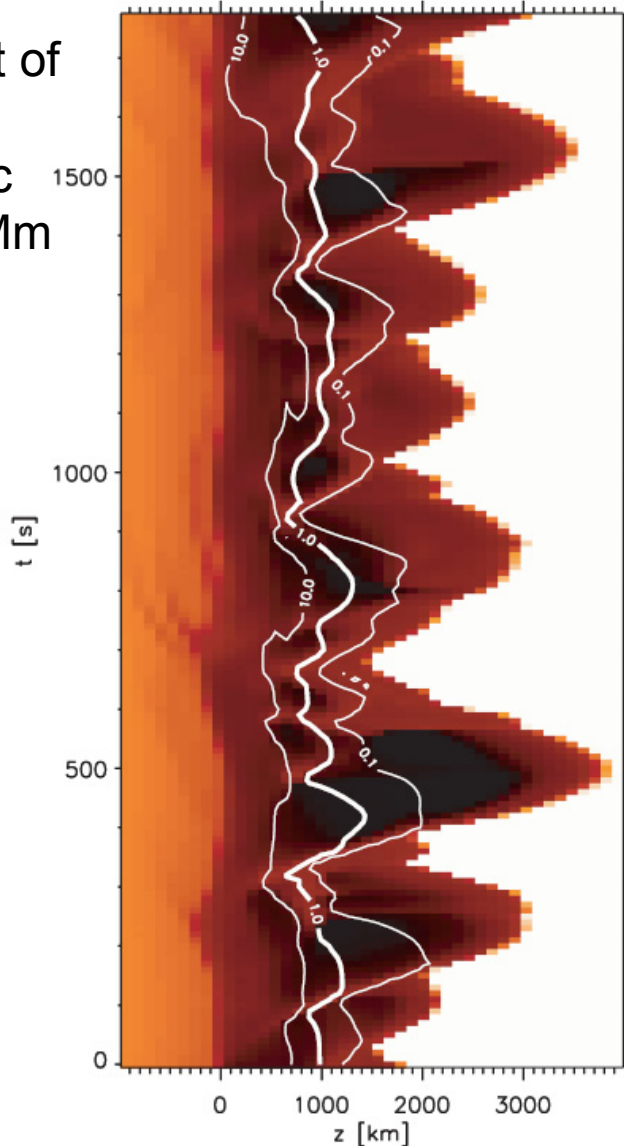
This gives strong support that fibrils are driven by magnetoacoustic shocks.

# Numerical 2-D MHD simulations of dynamic fibrils

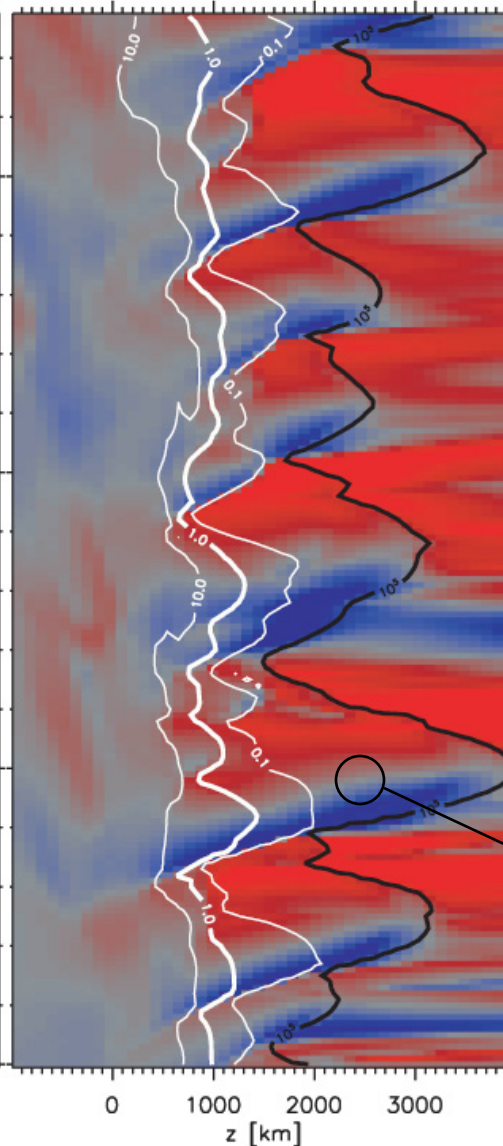


[De Pontieu et al. 2007: ApJ 655, 624](#)

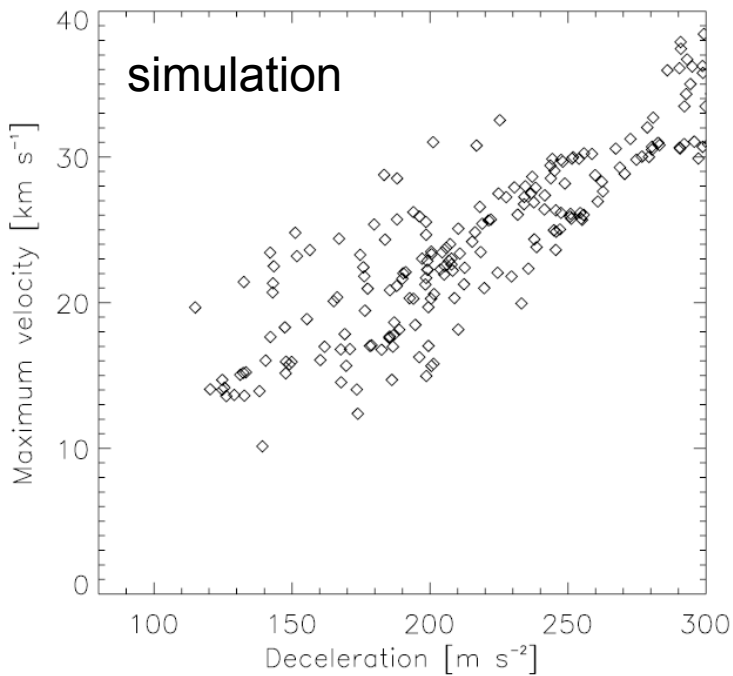
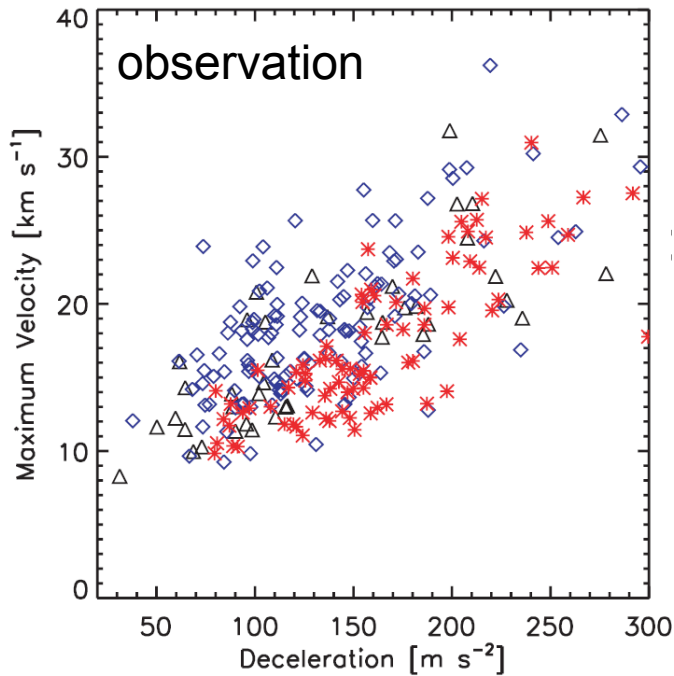
Time-slice plot of temperature within dynamic fibril at  $x = 4$  Mm



Time-slice plot of vertical velocity within dynamic fibril



# Numerical 2-D MHD simulations of dynamic fibrils



## Main results:

- striking similarities of observed and simulated values for deceleration, maximum velocity, maximum length, and duration of dynamic fibrils
- this strongly suggests that dynamic fibrils are formed by upwardly propagating waves generated in the photosphere as a result of p-mode oscillations

# Non-equilibrium hydrogen ionization in MHD simulations of the solar atmosphere

$$\frac{\partial \varrho}{\partial t} + \nabla \cdot (\varrho \mathbf{v}) = 0,$$

$$\frac{\partial \varrho \mathbf{v}}{\partial t} + \nabla \cdot \left[ \varrho \mathbf{v} \otimes \mathbf{v} + p_{\text{tot}} \underline{\underline{1}} - \frac{\mathbf{B} \otimes \mathbf{B}}{4\pi} \right] = \varrho \mathbf{g} + \nabla \cdot \underline{\underline{\tau}},$$

$$\frac{\partial e}{\partial t} + \nabla \cdot \left[ \mathbf{v}(e + p_{\text{tot}}) - \frac{1}{4\pi} \mathbf{B}(\mathbf{v} \cdot \mathbf{B}) \right] = \varrho(\mathbf{g} \cdot \mathbf{v})$$

$$+ Q_{\text{rad}} + \frac{1}{4\pi} \nabla \cdot (\mathbf{B} \times \eta \nabla \times \mathbf{B}) + \nabla \cdot (\mathbf{v} \cdot \underline{\underline{\tau}}) + \nabla \cdot (K \nabla T)$$

$$\frac{\partial \mathbf{B}}{\partial t} + \nabla \cdot [\mathbf{v} \otimes \mathbf{B} - \mathbf{B} \otimes \mathbf{v}] = -\nabla \times (\eta \nabla \times \mathbf{B}),$$

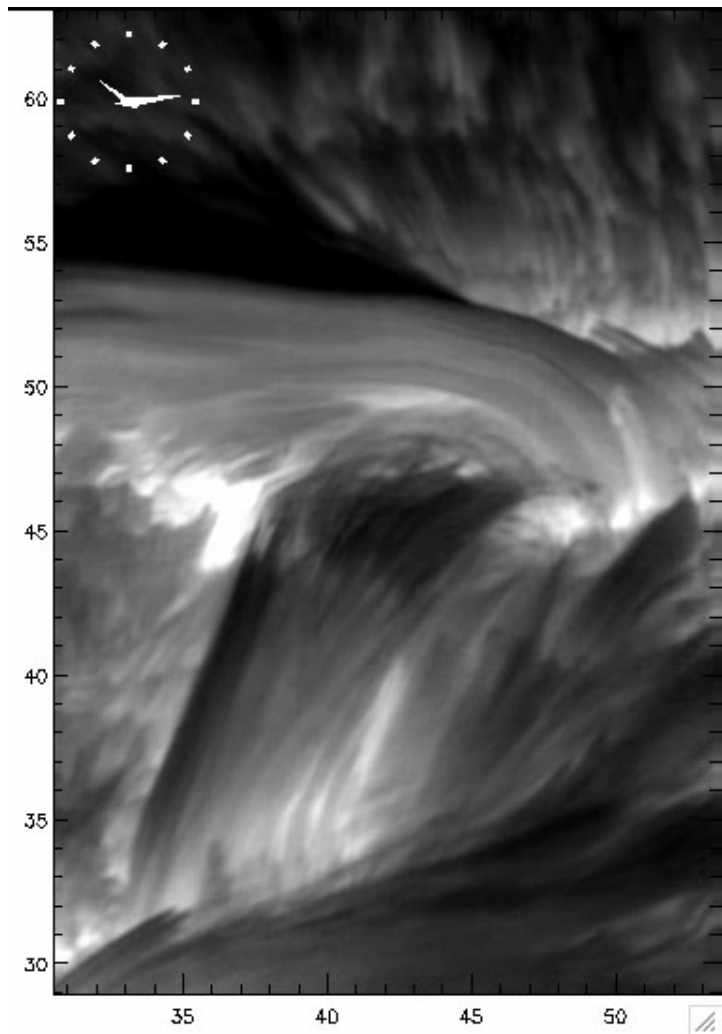
Radiative heating/cooling: 
$$Q_{\text{rad}} = 4\pi \varrho \int_{\nu} \kappa_{\nu} (J_{\nu} - B_{\nu}) \, d\nu.$$

$$\frac{\partial n_i}{\partial t} + \nabla \cdot (n_i \mathbf{v}) = \sum_{j,j \neq i}^{n_l} n_j P_{ji} - n_i \sum_{j,j \neq i}^{n_l} P_{ij}$$

+ equation of chemical equilibrium

+ equations of charge, internal energy, and particle (hydrogen nucleus) conservation

# Why non-equilibrium time-dependent hydrogen ionization ?



Since characteristic dynamic times of chromospheric fine structures are much shorter than time necessary to establish statistics equilibrium of hydrogen ionization.

In other words, the timescale on which the hydrogen level populations adjust to changes in the atmosphere is too long compared to the timescale on which the atmosphere changes.

Swedish 1-m Solar Telescope

diagnostics: H $\alpha$  line center

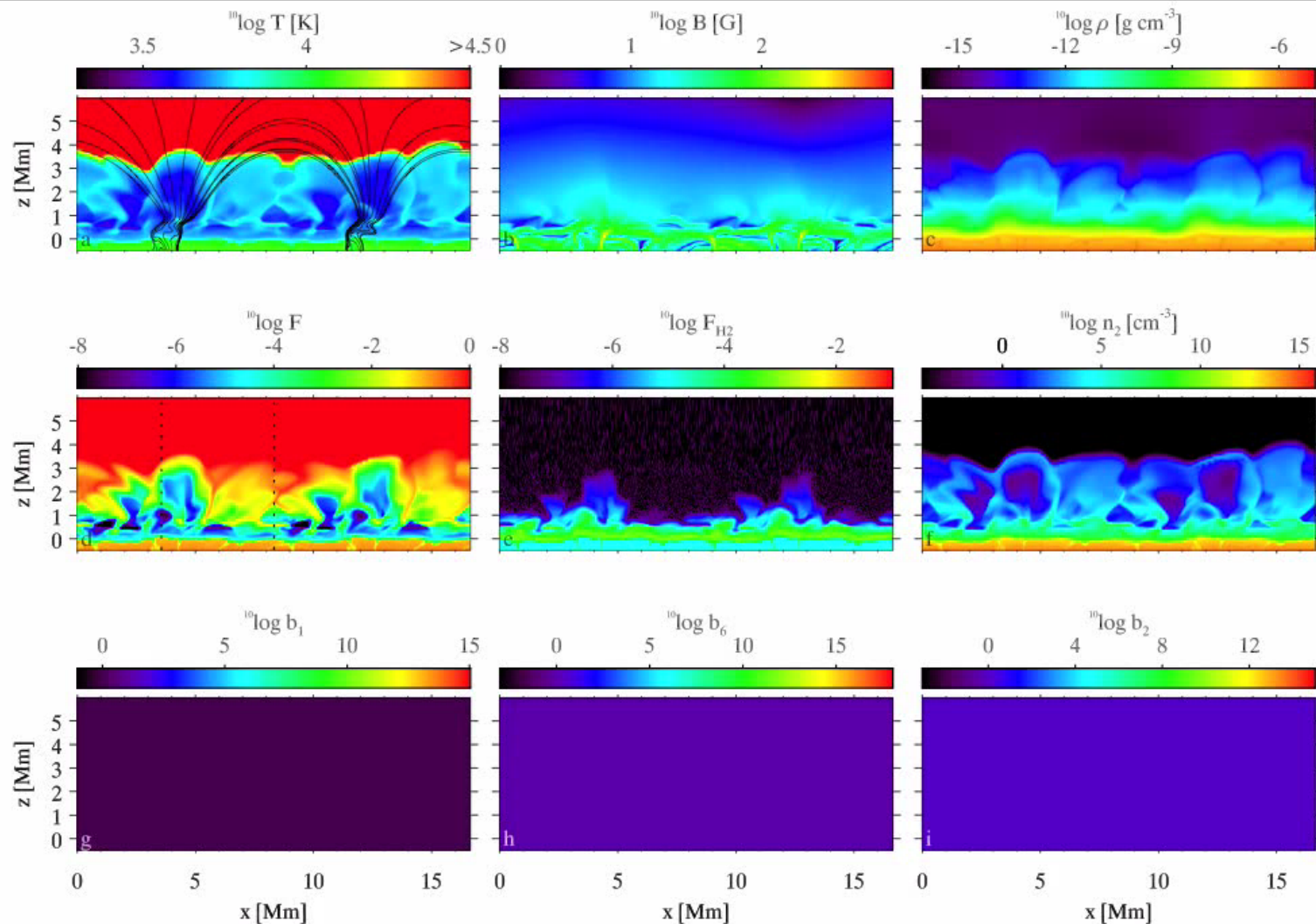
date: October 4, 2005

duration: 72 min

Resolutions - temporal : 3 frames per second

- spatial: ~ 70 – 100 km

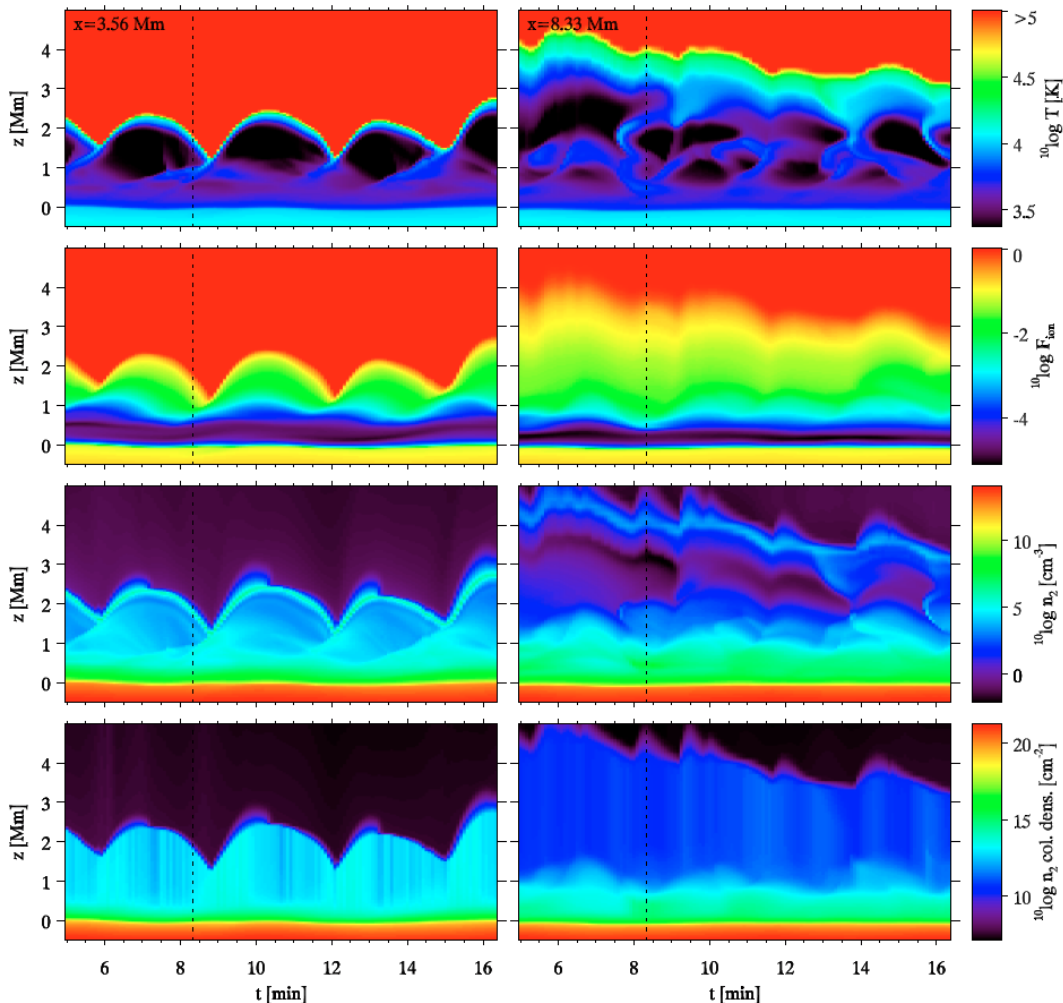
# Non-equilibrium hydrogen ionization in 2-D simulations of the solar atmosphere



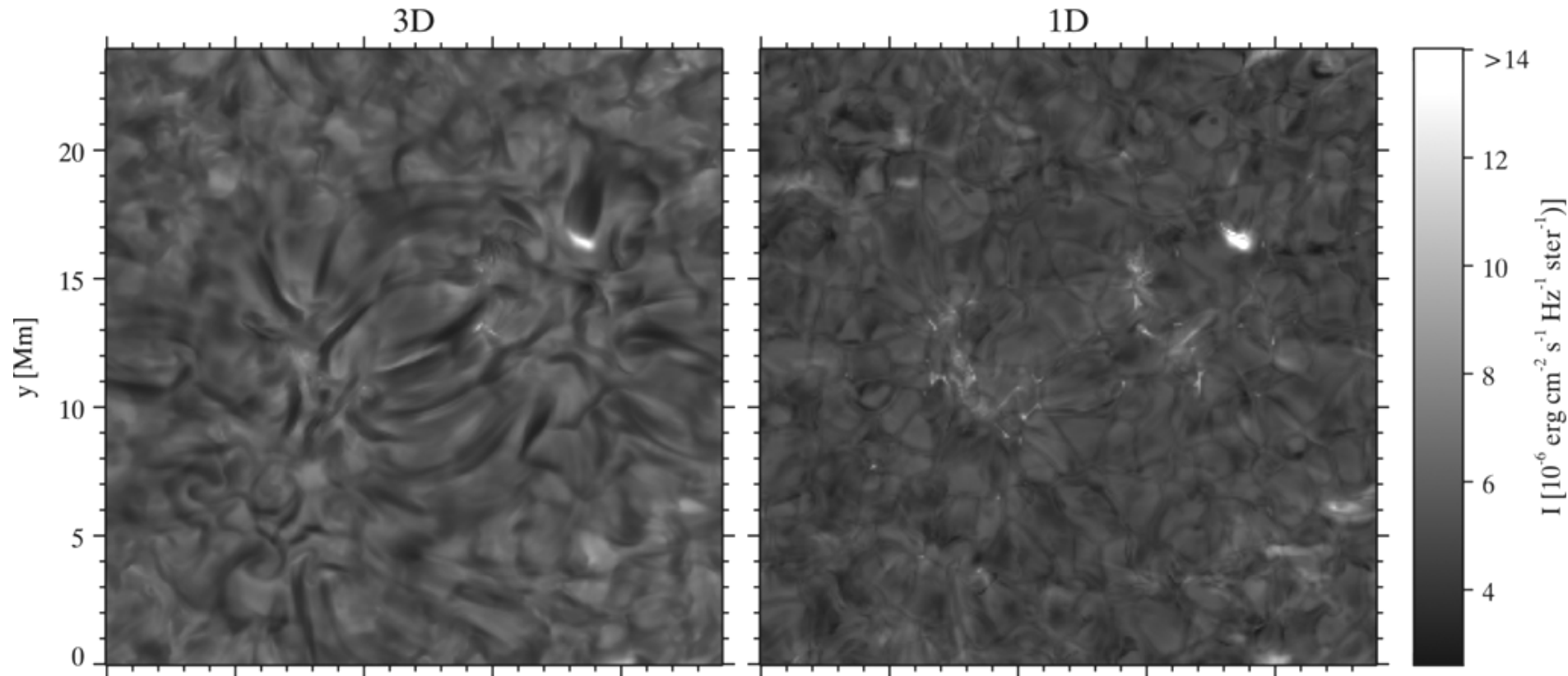
# Non-equilibrium hydrogen ionization in 2-D simulations of the solar atmosphere

## Main results:

- non-equilibrium H ionization is essential in simulations because the resulting temperature structure and hydrogen populations differ dramatically from their LTE values
- the degree of ionization of H in the chromosphere does not follow the local T
- the next step is to compute H $\alpha$  in detail from this simulation (not yet done)



# Fibril-like structures in numerical simulations of the chromosphere

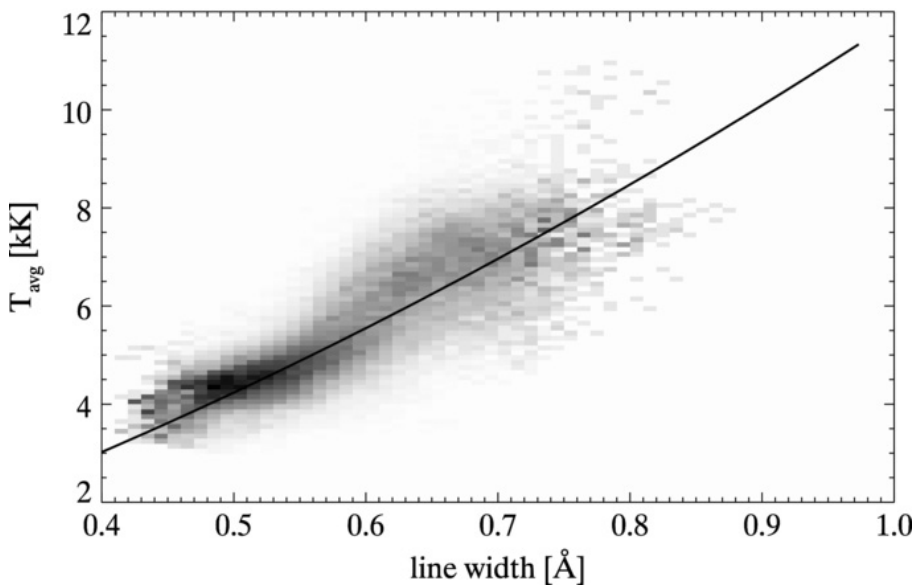


The formation of the H $\alpha$  line in the solar chromosphere

[Leenaarts et al. 2012: ApJ 749, 136](#)

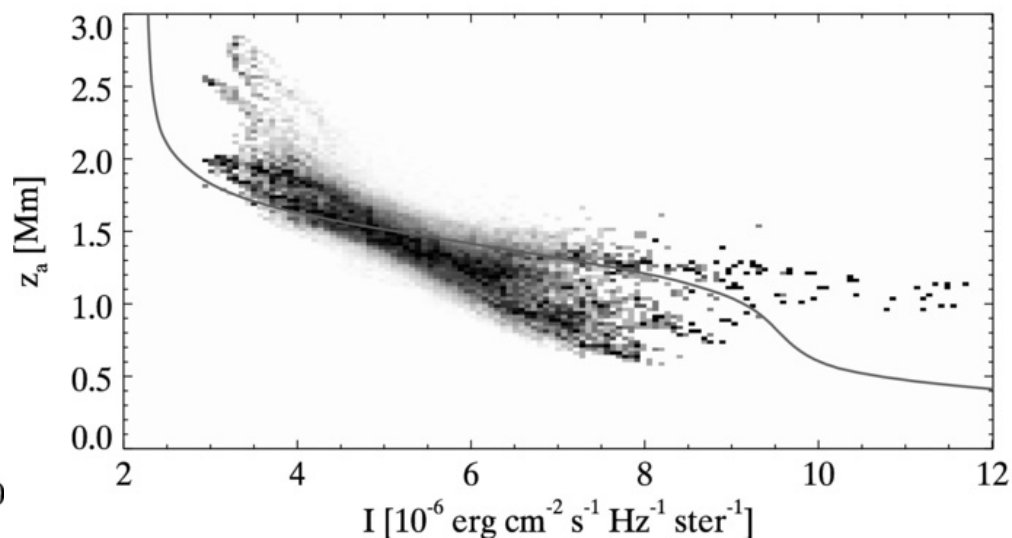
# The formation of the H $\alpha$ line in the solar chromosphere

the H $\alpha$  line width as a thermometer



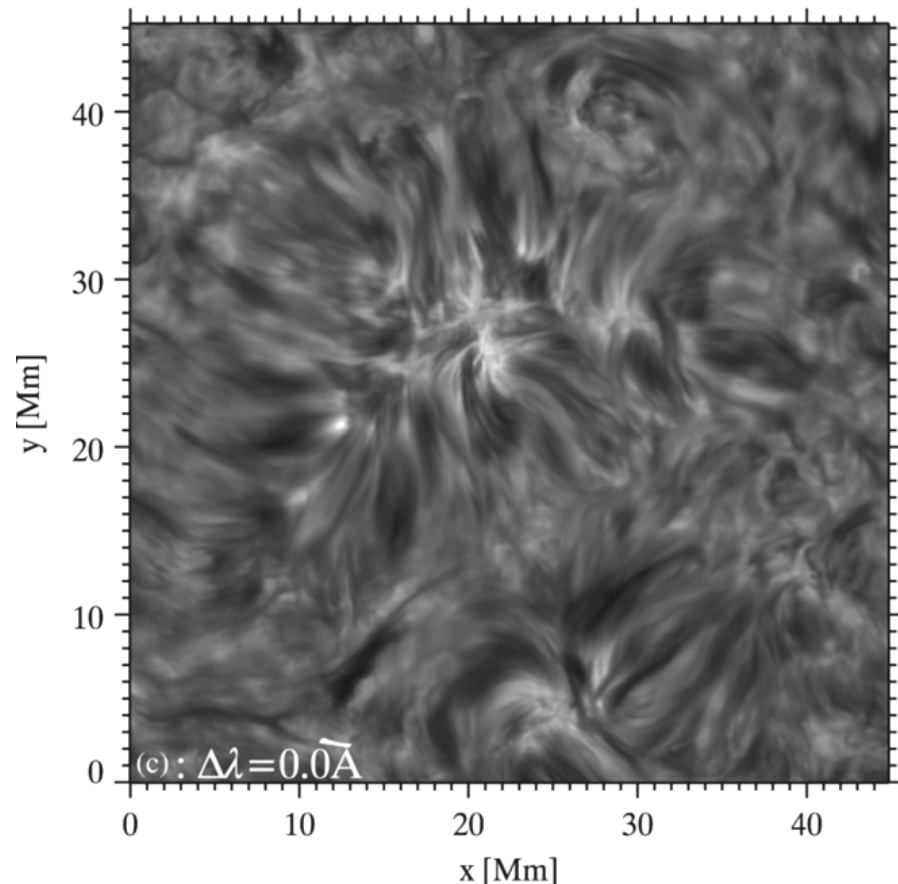
Temperature  $T_{\text{avg}}$  averaged between  $\tau = 0.5$  and  $\tau = 5$  at the wavelength of the profile minimum against the line-core width, after smoothing with a  $3 \times 3$  moving boxcar average.

the H $\alpha$  line center intensity as an indicator of formation height



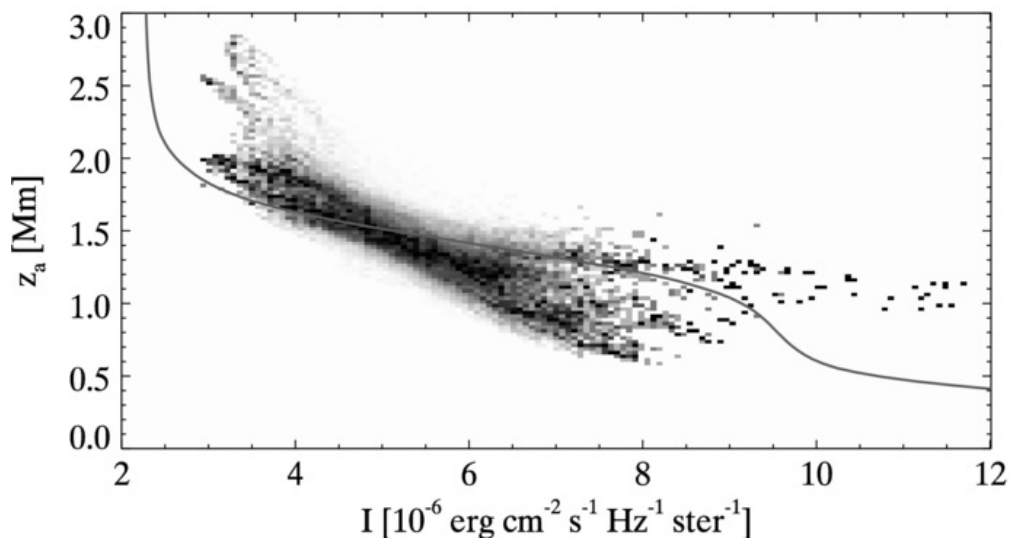
The average formation height  $z_a$  as a function of emergent H $\alpha$  intensity  $I$ .

# The formation of the H $\alpha$ line in the solar chromosphere



SST observation of H $\alpha$  in the line center.

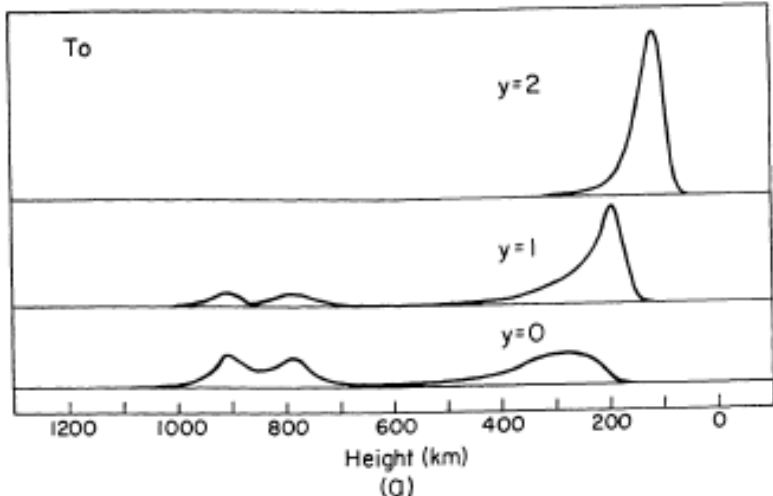
the H $\alpha$  line center intensity as  
an indicator of formation height



The average formation height  $z_a$  as  
a function of emergent H $\alpha$  intensity  $I$ .

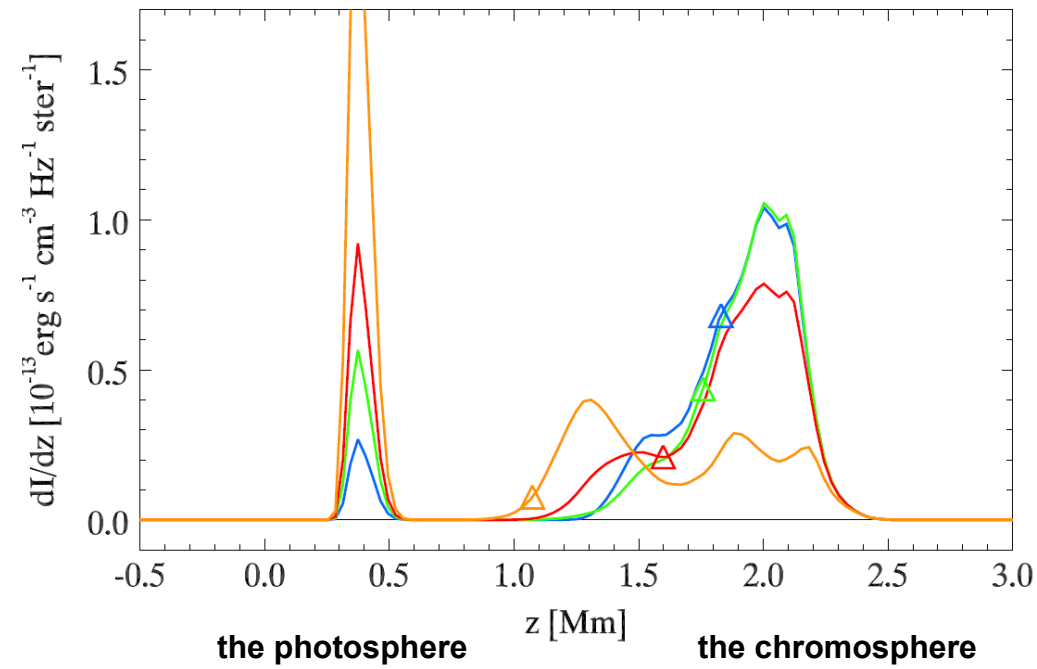
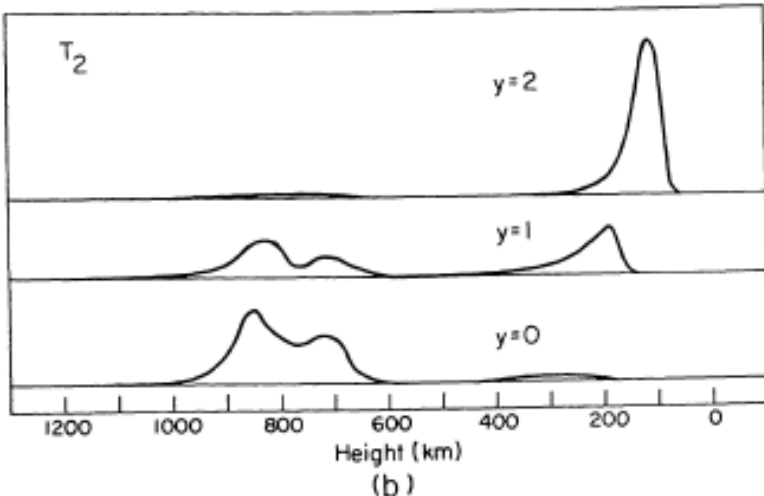
Result of numerical simulation.

# Double-peak contribution function of the H $\alpha$ line



the chromosphere

the photosphere



# Take-away summary of the H $\alpha$ line properties

- no reversed granulation observed in the H $\alpha$  wing images
- double-peak contribution function
- sensitive thermometer, line width – temperature correlation
- negative correlation of the center intensity and the formation height
- not quiet ideal spectropolarimetric diagnostics, sensitive to everything (López Ariste, private communication)